

**FABRICATION AND CHARACTERIZATION OF
PERYLENE DIIMIDE DOPED POLYFLUORENE
BASED SOLUTION PROCESSED BLUE ORGANIC
LIGHT EMITTING DIODES**

**A Thesis Submitted to
the Graduate School of Science of
İzmir Institute of Technology
in Partial Fulfillment of the Requirements for the Degree of
MASTER OF SCIENCE
in Photonics Science and Engineering**

**by
Sevde Nur UTLU**

**December 2023
İZMİR**

We approve the thesis of **Sevde Nur UTLU**

Examining Committee Members:

Prof. Dr. Canan VARLIKLI

Photonics Science and Engineering/Izmir Institute of Technology

Prof. Dr. Cem ÇELEBİ

Physics/Izmir Institute of Technology

Prof. Dr. Ceylan ZAFER

Solar Energy/Ege University

11 December 2023

Prof. Dr. Canan VARLIKLI

Supervisor, Photonics Science and Engineering/Izmir Institute of Technology

Prof. Dr. Mustafa M. DEMİR

Co-Supervisor, Materials Science and Engineering/Izmir Institute of Technology

Prof. Dr. Canan VARLIKLI

Head of The Department of Photonics Science and Engineering/Izmir Institute of Technology

Prof. Dr. Mehtap EANES

Head of The Graduate School of Engineering and Science/Izmir Institute of Technology

ACKNOWLEDGEMENTS

First and foremost, I would like to express my gratitude to my advisor, Prof. Dr. Canan VARLIKLI, for her unwavering support and guidance throughout my master's studies.

I would like to thank to my co-advisor Prof. Dr. Mustafa M. DEMİR and committee members Prof. Dr. Ceylan ZAFER and Prof. Dr Cem ÇELEBİ for their participation and comments.

I also extend my heartfelt thanks to my former groupmate, Volkan BOZKUŞ, who never hesitated to support me in adapting to the laboratory and work conditions while conducting my research. I am deeply grateful to Hakan Bozkurt for his prompt assistance at any time, even in the face of immediate problems. Special thanks to my lab mate, Dr. Erkan AKSOY, for his comments on my thesis, contributions, and permission to use the synthesized molecules. I would also like to express my sincere thanks to my friend Metin TAN.

I am deeply thankful to my family for their constant support and trust in me. I am particularly grateful to my husband, Yasin UTLU, for motivating me during my hectic schedule. I appreciate his gentle guidance and understanding during moments of panic and stress.

This work was supported by Scientific and Technological Research Council of Turkey (TÜBİTAK, Project Number: 119F031)

ABSTRACT

FABRICATION AND CHARACTERIZATION OF PERYLENE DIIMIDE DOPED POLYFLUORENE BASED SOLUTION PROCESSED BLUE ORGANIC LIGHT EMITTING DIODES

Blue is considered as the major component in many applications of organic light emitting diodes (OLEDs). Most of the polymeric BEs including poly[9,9-di-(2-diethylhexyl)-fluorenyl-2,7-diyl] (ADS231BE) attract attention with their solubility and potential in reducing the application costs, but also suffer from wide electroluminescence resulting in color purity issues. Annealing temperature and solvent choice have great influence on morphology and electronic properties. A typical OLED is fabricated by using ADS231BE as the emitter material and effect of annealing temperature on EL properties is investigated between 60°C and 150°C. OLEDs produced using toluene have shown better efficiency compared to those using chlorobenzene. Regardless of the solvent used, the efficiencies gradually decreased, but the stability and color purity of the devices increased with increasing annealing temperatures. Surface morphologies were examined, and suitable coating conditions were determined.

Small molecule orange-red-emitting N,N'-bis(2-ethylhexyl)perylene-3,4,9,10-dicarboxylic diimide (PDI) derivatives were introduced into the blue-emitting conjugated polymer ADS231BE at a concentration of 0.1 wt.%. Electroluminescence, morphology, photoluminescence and Raman analysis of the developed devices were completed to determine the type of aggregation and conformational change caused by PDI doping. Subsequently, to balance charge and improve the electroluminescent character of the devices, a hole transfer layer (HTL) consisting of Poly (N-vinyl carbazole) (PVK) and PVK:1,3-Bis(N-carbazolyl) benzene (mCP) was added to the device structure. Similar morphological and Raman analyses were performed. Compared to the bare ADS231BE containing devices, without changing the CIE coordinate values, approximately, 10 folds of luminance and more than 5 folds of EQE increments were obtained.

ÖZET

ÇÖZELTİ SÜREÇLİ, PERİLEN DİİMİD KATKILI, POLİFLOREN TABANLI MAVİ IŞIK YAYAN ORGANİK DİYOTLARIN HAZIRLIĞI VE KARAKTERİZASYONU

Mavi, organik ışık yayan diyotların (OLED'ler) birçok uygulamasında ana bileşen olarak kabul edilir. Polimerik mavi emisyon yapan maddelerin çoğu, poli[9,9-di-(2-diethylhexyl)-fluorenyl-2,7-diyl] (ADS231BE) dahil, çözünürlükleri ve uygulama maliyetlerini azaltma potansiyelleri nedeniyle dikkat çeker, ancak geniş elektrolüminesans (EL) nedeniyle renk saflığı sorunlarıyla karşılaşılır. Tavlama sıcaklığı ve çözgen seçimi, morfoloji ve elektronik özellikler üzerinde büyük bir etkiye sahiptir. Yayıcı malzemesi olarak ADS231BE kullanılarak, tipik bir OLED üretilmiştir ve 60°C ile 150°C arasındaki tavlama sıcaklığının EL özellikleri üzerindeki etkisi incelenmiştir. Tolüen kullanılarak üretilen OLED'ler, klorobenzen kullanılanlara kıyasla daha iyi verimlilik göstermiştir. Kullanılan çözümden bağımsız olarak, verimlilik değerleri giderek azalırken, tavlama sıcaklığının artmasıyla cihazların kararlılığı ve renk saflığı artmıştır. Yüzey morfolojileri incelenerek, uygun kaplama koşulları belirlenmiştir.

Mavi ışık yayan konjuge polimer ADS231BE içerisine, küçük molekül turuncu-kırmızı ışık yayan N,N'-bis(2-ethylhexyl)perylene-3,4,9,10- dicarboxylic diimide (PDI) türevleri kt. %0.1 katkı olarak Förster tipi enerji transferi için kullanılmıştır. Geliştirilen aygıtların elektrolüminesans, morfoloji, fotolüminesans ve Raman gibi incelemeleri yapılmıştır ve PDI katkılmasının sebep olduğu “yığılma” tipi ve konformasyonel değişim tespit edilmiştir. Ardından aygıt yapısına, yük dengesini sağlamak ve aygıtların elektrolüminesans karakterini geliştirmek için boşluk transfer katmanı (HTL) olarak Poly(N-vinylcarbazole)(PVK) ve PVK 1,3-Bis (N-carbazolyl) benzene eklenmiştir. Benzer şekilde morfoloji ve Raman analizleri gerçekleştirilmiştir. Yalnızca ADS231BE içeren aygıtlarla karşılaştırıldığında, CIE koordinat değerleri değiştirilmeden, parlılık değerlerinde yaklaşık 10 kat ve EQE değerinde 5 kattan fazla artış elde edilmiştir.

To my parents and my dearest spouse ...

TABLE OF CONTENTS

LIST OF FIGURES	ix
LIST OF TABLES.....	xi
LIST OF SYMBOLS AND ABBREVIATIONS	xii
CHAPTER 1. INTRODUCTION.....	1
1.1. Importance of OLEDs.....	2
1.1.1. Blue OLEDs.....	6
1.2. Aim of The Thesis	8
1.3. Experimental	8
1.3.1. Materials	8
1.3.2. Instruments.....	9
1.3.3. Fabrication of Devices.....	10
CHAPTER 2. THE FABRICATION OPTIMIZATION OF SOLUTION PROCESS POLYFLUORENE BASED BLUE OLEDs	11
2.1. Importance of Polyfluorene Based Blue Organic Light Emitting Diodes	11
2.2. Performances Polyfluorene Based and Perylene Diimids Doped Polyfluorene Based OLEDs.....	15
2.3.1. Devices Characteristic	16
2.3.2. Morphology Analysis	21
2.3.3. Photophysical Analysis.....	22
CHAPTER 3. DEVICE PERFORMANCE OF POLYFLUORENE BASED AND PERYLENE DIIMID DOPED POLYFLUORENE BASED BLUE OLEDs.....	23
3.1. Importance of Polyfluorene Based Perylene Diimid Doped Blue Organic Light Emitting Diodes.....	24
3.1.1. Perylene diimids based OLEDs.....	25
3.1.2. Device Characteristics	27
3.1.3. Morphological Analysis	30
3.1.4. Photophysical Analysis.....	32
3.1.5. Raman Spectroscopy Analysis	33
3.2. Polyfluorene Based and Perylene Diimid Doped Polyfluorene Based OLEDs with HTLs	35
3.2.1. Devices Characteristic	38

3.2.2. Morphological Analysis	41
CONCLUSION.....	43
LIST OF REFERENCES.....	44
APPENDIX A.....	54

LIST OF FIGURES

<u>Figure</u>	<u>Page</u>
Figure 1.1. Side section of conventional organic light emitting diode (Lighting Equipment Sales, n.d.).	5
Figure 1.2. CIE 1931 chromaticity diagram (MSI 2019).	6
Figure 1.3. Chemical structures of some blue polymer emitters, poly-(para-phenylene) (PPP), poly(9,9-dihexylfluorene-alt-co2,5-didecyloxy-para-phenylene) (PDHFDDOP), polyfluorene (PFO), respectively.	7
Figure 1.4. Top-side scheme of the fabricated devices.	10
Figure 2.1. Chemical structure of purchased ADS231BE (“ADS231BE,” n.d.).	15
Figure 2.2. Energy band diagram and device structure of the fabricated devices with bare BE layer.	17
Figure 2.3. a, b, and c) external quantum efficiency vs current density and d, e and f) normalized electroluminescence vs wavelength at maximum luminescence characteristics of devices prepared by coating with chlorobenzene and toluene solvent and annealed at different temperatures in air and N ₂ atmosphere, respectively.	18
Figure 2.4. Represent of PL and Abs spectrums of BE active layers at 380 nm excitation wavelength thin film spectra.	22
Figure 3.1. Chemical structure of synthesized perylene derivatives PDI(2EH)-ref and PDI(2EH)-1 by Erkan Aksoy (Aksoy 2020).	26
Figure 3.2. Energy band diagram and device structure of the fabricated devices with PDIs doped emissive layers.	28
Figure 3.3. a) and d) current density, b) and e) luminance vs applied voltage and c) and f) normalized electroluminescence vs wavelength at maximum luminescence characteristics of devices prepared by BE and PDIs doped BE emissive layer. a, b, c at 75°C and d, e, f at 150°C, respectively.	29
Figure 3.4. Represent of a) Photo luminance spectrum and b) Absorbance spectrum of solid-state thin films of active layers excited at 380 nm.	32
Figure 3.5. Solid state Raman spectra in the high wavenumber region between a)1550-1650 cm ⁻¹ , b) 1100-1500 cm ⁻¹ and c) in the low wave number region 300-1100 cm ⁻¹ all active layer without HTL layers.	34
Figure 3.6. Chemical structure of 1,3-bis(carbazol-9-yl) benzene (mCP) and Poly(N-vinylcarbazole) (PVK)	36
Figure 3.7. Energy band diagram and device architecture of the fabricated devices.	38

<u>Figure</u>	<u>Page</u>
Figure 3.8. a) and d) current density, b and e) luminance vs applied voltage and c and f) normalized electroluminescence vs wavelength at maximum luminescence characteristics of devices prepared by BE and PDIs doped BE emissive layer and PVK and PVK: mCP hole transport layers.	39
Figure 3.9. CIE coordinates of fabricated devices.....	40

LIST OF TABLES

<u>Table</u>	<u>Page</u>
Table 2.1. Literature view of polyfluorene based blue organic light emitting diodes....	14
Table 2.2. Electroluminescence efficiencies of the devices annealed at gradually increased temperatures and prepared by coating with chlorobenzene and toluene solvents in air and N ₂ atmosphere.	19
Table 2.3. x, y coordinate values of devices with BE active layer annealed at 125°C and 150°C varying with applied voltage.	20
Table 2.4. AFM images were obtained of BE films spin-cast at 2000rpm on mica substrates using CB and Tol solvents at temperatures of 75°C and 150°C. ..	21
Table 3.1. Electroluminescence efficiencies of the BE and PDIs doped BE devices.....	30
Table 3.2. AFM images of a) ADS231BE b) PDIref doped 0.1 %wt. BE and c) PDI1 doped 0.1 %wt. BE thin films spin casting in mica substrate at 3000rpm-min with 10mg/mL toluene and annealed at 150°C. And d, e, f are 3D images of their, respectively.....	31
Table 3.3. Electroluminescence efficiencies were evaluated for BE and PDIs-doped BE layers as emissive layer and PVK and PVK:mCP layers as hole transport layer.....	40
Table 3.4. AFM images of PDIref doped PFO-POSS based OLEDs with HTLs.	42

LIST OF SYMBOLS AND ABBREVIATIONS

Abs	Absorption
AFM	Atomic Force Microscopy
ADS231BE	POSS group ended Poly(9,9-dioktilfluorenil-2,7-diil)
BE	Blue Emitter
CIE	Commission Internationale de l'éclairage
Cs ₂ CO ₃	Cesium Carbonate
EIL	Electron Injection Layer
EL	Electroluminescence
EML	Emissive layer
EQE	External quantum efficiency
FWHM	Full width at half maximum
HCl	Hydrochloric acid
HOMO	Highest Occupied Molecular Orbital
ITO	Indium tin oxide
LUMO	Lowest Unoccupied Molecular Orbital
mCP	1,3-Bis (N-carbazolyl) benzene
OLED	Organic Light Emitting Diode
PDI	N ² -bis(2-ethylhexyl)perylene-3,4,9,10-dicarboxylic diimide
PEDOT:PSS	Poly(3,4-ethylenedioxythiophene):poly(styrene sulfonate)
PFO	Polyfluorene
PL	Photoluminescence
POSS	Polyhedral oligomeric silsesquioxane
PVD	Physical Vapor Deposition
PVK	Poly (N-vinyl carbazole)
Ra	Roughness average
RPM	Rounds per minutes
SCLC	Space charge limited current
UV-vis	Ultraviolet-visible
WOLED	White Organic Light Emitting Diode
Å	Angstrom
Al	Aluminum

Au	Gold
Tol	Toluene
CB	Chlorobenzene
CuPc	Copper Phthalocyanine
E	Electric Field
ϵ	Electrical permittivity of material
ϵ_0	Electrical permittivity of free space
μ	Mobility
μ_0	Zero-field mobility
D	Thickness
J	Current Density
B	Poole-Frenkel factor
V	Voltage
wt.	Weight
Λ	Wavelength
Nm	Nanometer
Cm	Centimeter

CHAPTER 1

INTRODUCTION

The historical development of organic optoelectronics and organic semiconductors fundamentally revolves around the discovery of the electronic and optical properties of organic materials and the subsequent integration of these properties into a broader range of applications. The continuous advancements in this field are crucial for the exploration of more sustainable and flexible solutions in electronic and optical technologies.

The history of organic semiconductors can be traced back to experimental investigations into the electrical conductivity properties of organic materials in the 1920s (Birks, Appleyard, and Pope 1936). Studies carried out on specific organic compounds in this period indicated the possible semiconductor characteristics inherent in these materials. The 1950s witnessed the development of the first organic semiconductor transistors (Birks, Appleyard, and Pope 1936). While the semiconductor transistor was originally invented by William Shockley, John Bardeen, and Walter Brattain at Bell Laboratories in 1947, the exploration of transistors utilizing organic semiconductors required additional time for fruition (Shannon 1948).

Significant strides were made in the field of organic electronics during the 1970s. Research endeavors focusing on the integration of organic semiconductors into electronic devices gained momentum (Moliton and Hiorns 2012; Drexler 2004). In 1980s and 1990s period witnessed pivotal advancements in the synthesis and characterization of organic semiconductor materials. Various synthesis and processing methodologies were developed to enhance the efficiency and stability of organic materials. Organic optoelectronics received heightened interest in the 1980s as researchers focused on merging the optical and electronic properties of organic materials. The research during this period focused on the light emission and other optical properties of organic semiconductors. The 20th later century witnessed a major milestone in the development of organic optoelectronic devices, specifically organic light-emitting diodes (OLEDs). Tang produced the first organic p–n junction solar cell from the p-type CuPc in 1986. The origins of OLED technology date back to 1987 when two researchers at Kodak, Steven

Van Slyke and Ching Tang, obtained patents that described OLEDs utilizing organic materials (Tang and Vanslyke 1987).

The commercial potential of organic semiconductors is significant, particularly in the development of thin, lightweight, and flexible displays. The 2000s witnessed the practical application of organic semiconductors, leading to the emergence of novel organic optoelectronic devices, such as organic photovoltaic cells. During this period, organic semiconductors started to be utilized in various fields, including energy production, storage, flexible electronics, and wearable technology.

Ongoing research continues to propel the investigation of organic semiconductors, and these materials find applications in diverse fields such as flexible electronics, wearable technology, energy storage, and beyond. Organic electronics represent an alternative approach to traditional silicon-based electronics (Vavilov 1994). Organic optoelectronics persist, with the application areas of organic semiconductors gradually broadening. Presently, ingenious uses including flexible displays, smart textiles, and biosensors are notable in the modern sphere of organic optoelectronics (Ostroverkhova 2016; Jihun Park et al. 2017; Shaw and Seidler 2001).

1.1 Importance of OLEDs

Organic Light-Emitting Diodes, commonly known as OLEDs, play a pivotal role in various applications owing to their distinctive features and advantages. Unlike conventional liquid crystal displays (LCDs), OLEDs emit light directly when an electric current passes through them, eliminating the need for a separate backlight. This unique characteristic allows OLEDs to achieve superior contrast ratios, delivering brighter and more saturated colors for an enhanced picture quality. The organic materials used in OLEDs possess inherent flexibility, enabling the creation of innovative form factors like flexible and rollable displays, curved screens, and bendable devices.

Moreover, OLED displays are characterized by their thin and lightweight nature compared to traditional display technologies. This slim profile is particularly advantageous in settings that prioritize compactness and lightness, such as portable electronic devices and wearable technology. OLEDs are inherently more efficient than traditional illumination methods, providing precise regulation of brightness levels with

individual pixel illumination. Inactive pixels consume no energy, contributing to energy conservation in display applications (Sasabe and Kido 2013).

Prototypes of the first color OLED displays emerged during this period, initially for small screens. In 2003, Sony introduced the world's first commercially available OLED television. This marked the potential for OLED technology to be used in large-screen consumer electronics applications. The first smartphones featuring OLED displays were introduced in 2008. Samsung released two models, the Samsung i7110 and Samsung Omnia, showcasing OLED displays in mobile devices (Alsop, n.d.; Hong et al. 2021).

OLEDs offer exceptional viewing angles, maintaining consistent color and brightness even when viewed from off-angles. This makes them ideal for applications where diverse audiences may view the screen from different perspectives. Additionally, OLEDs boast a fast response time, a crucial attribute in fields like gaming and virtual reality, where rapid responses enhance user immersion. The technology also enables the development of transparent displays, facilitating augmented reality and heads-up displays that provide information without obstructing the view of user. In summary, OLEDs represent a versatile and advanced display technology with numerous benefits across various industries (Jadoun and Riaz 2020).

Organic materials utilized in OLEDs are more ecologically friendly than some inorganic materials employed in other display technologies. Moreover, the capability for reducing energy consumption in OLED lighting applications is a key contributor to their favorable environmental impact. They have been applied in numerous industries, among them consumer electronics (including smartphones and TVs), automotive displays, lighting, and healthcare. The adaptable nature and distinctive characteristics of OLED technology encourage further development in display and lighting solutions, classifying it as a significant and influential technology in the contemporary technological world.

OLED devices consist of several layers that work together to produce light and form a process referred to as electroluminescence. The basic layers and working principle of OLED devices are substrate, electrodes and organic carrier transport layers. The substrate serves as the base layer of the OLED device. It is typically made of glass or a flexible material like plastic, depending on the application. Positioned on top of the substrate, the anode layer is a transparent, conductive layer. It facilitates the flow of positive charge carriers, often referred to as "holes". The organic layers are the central components that emit light when an electric current is applied. There are typically three main organic layers Hole Transport Layer (HTL), Emissive Layer (EML) and Electron

Transport Layer (ETL). HTL, facilitates the movement of positive charges (holes) from the anode. EML is where light is generated. The organic compounds in this layer determine the color of the emitted light. Red, green, and blue are common colors used in combination to produce a full spectrum. ETL, facilitates the movement of negative charges (electrons) from the cathode. The cathode layer is, conductive layer positioned on top of the organic layers. It injects electrons into the organic layers, completing the electrical circuit necessary for light emission. For efficient hole injection in OLED systems, one can utilize a hole injection layer (HIL) suitable to HOMO energy levels. PEDOT:PSS is one of the most commonly used HIL materials. It is a water-based solution that effectively smooths out the ITO surface, thereby preventing potential electrical short, reducing the operating voltage, and increases life of the device (Brown et al. 1999). In OLED devices, the total current is determined by the holes due to the fact that the HTL have the efficient hole transmission property and high hole transport speed. Hole transport speed (mobility) of HTL generally vary between 10^{-3} and 10^{-4} $\text{cm}^2/\text{V}\cdot\text{s}$. A suitable HTL material must exhibit morphological stability and form a uniform thin film when coated, possess a low ionization potential, feature high hole transport speed, and exhibit low electron attraction. This stability is essential for the reliability and longevity of the devices. Another layer, the ETL materials should be morphologically stable and form uniform thin film when coating, have high ionization potential, have high electron transport speed and have high electron attractiveness. The electron transport speed in the material varies depending on the electric field and is approximately 10^{-5} to 10^{-2} $\text{cm}^2/\text{V}\cdot\text{s}$.

The EML materials are often classified into different categories based on the color of light they emit. The three primary colors used in OLED displays are red, green, and blue. Some of the commonly used small molecules are **Alq3** (Tris(8-hydroxyquinolino)aluminum), often used as a green emitter, **PDI** (Perylenediimid) is used as a red emitter and **Ir(ppy)2(acac)** (Tris[2-(p-tolyl)pyridinato-C2,N]iridium(III)) is used as a blue emitter (BE). The Polymeric materials are **MEH-PPV** (Poly[2-methoxy-5-(2'-ethylhexyloxy)-1,4-phenylenevinylene]) used as a red emitter and **PFO** (Poly(9,9-dioctylfluorene)) used as a BE.

When a voltage is applied across the anode and cathode, an electric field is created in the organic layers. This electric field facilitates the movement of electrons from the cathode and holes from the anode. Electrons and holes recombine in the emissive layer. As they recombine, energy is released in the form of light. The color of the light is determined by the organic compounds in the emissive layer. OLED light color use a

combination of red, green, and blue organic compounds in the emissive layer to produce a full range of colors and it is reached white light emitting (Figure 1.1).

The operation of OLEDs is governed by principles of device physics and charge transport mechanisms. OLEDs consist of multiple organic layers sandwiched between an anode and a cathode. These layers include a HTL, an EML, and an ETL. Energy levels of these layers are critical. The energy levels of the **HOMO** (Highest Occupied Molecular Orbital) and **LUMO** (Lowest Unoccupied Molecular Orbital) of the materials must be appropriately aligned to ensure efficient charge injection and recombination.

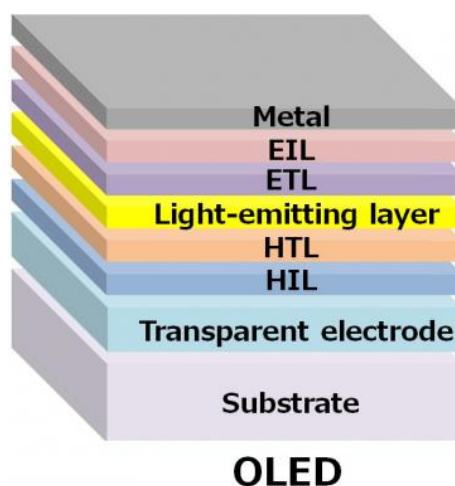


Figure 1.1. Side section of conventional organic light emitting diode (Lighting Equipment Sales, n.d.).

When a voltage is applied across the OLED, electrons are injected from the cathode into the **ETL**, and holes are injected from the anode into the **HTL**. These charge carriers move toward each other and recombine in the emissive layer to form excitons. Excitons, which are bound electron-hole pairs, can migrate within the **EML** before undergoing radiative decay to emit light. The distance excitons can travel before recombination depends on factors like the material properties and the applied electric field. Efficient radiative recombination of excitons in the **EML** results in the emission of light. The color of the emitted light is determined by the energy bandgap of the materials in the emissive layer. Non-radiative processes, such as triplet-triplet annihilation and exciton-polaron quenching, can compete with radiative recombination, affecting the overall efficiency of the device.

The charge transport mechanism in OLEDs, basically holes move through the HTL toward the EML. Electrons move through the ETL toward the EML. Achieving

balanced charge transport is crucial for maximizing device efficiency. The choice of HTL and ETL materials is essential for maintaining this balance. The region where holes and electrons recombine to form excitons is known as the recombination zone. The position and width of this zone impact the efficiency and color purity of the emitted light.

1.1.1 Blue OLEDs

White light is typically emitted by combining blue, green, and red emitters within a single OLED device. The approach involves mixing emissions from different color emitters to generate a broad-spectrum white light. Currently, generating white light in LEDs typically entails phosphor conversion or the combination of multiple color-emitting LEDs (Figure 1.2). The BE is a crucial component in the generation of white light in White Organic Light Emitting Diodes (**WOLEDs**). Blue emission serves as the primary source, and the challenge is to produce a stable and efficient BE.

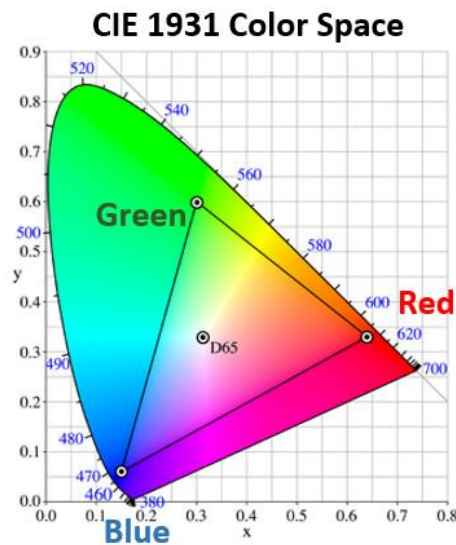


Figure 1.2. CIE 1931 chromaticity diagram (MSI 2019).

The initial blue LED was produced using poly-(para-phenylene) (PPP). Subsequently, soluble PPP derivatives were synthesized and utilized to exhibit blue Polymer Light Emitting Diodes (**POLEDs**). In recent years, 9,9-disubstituted polyfluorenes (**PFO**) have gained significant importance as blue electroluminescence (**EL**) materials. Then, Yu et.al, report a blue EL polymer, poly(9,9-dihexylfluorene-alt-co2,5-didecyloxy-para-phenylene) (PDHFDDOP), and they describe initial results

obtained from PLEDs made from this polymer (Yu et al. 1999; Ohmori et al. 1991) shown in Figure 1.3.

Producing a stable and efficient BE in OLEDs presents several challenges compared to red and green emitters. Blue light has a higher energy level compared to red and green light. Achieving efficient blue emission requires materials with a larger energy gap between the HOMO and the LUMO. Designing materials with a suitable energy gap is challenging and often involves a trade-off between stability and efficiency. The molecular design of blue-emitting materials is often more complex due to the need for specific electronic and structural characteristics. Designing molecules that simultaneously possess high electron affinity, high hole mobility, and good thermal stability is challenging. Blue-emitting materials are often more sensitive to environmental factors such as oxygen and moisture. Degradation reactions, such as photooxidation, can occur more readily in BEs, leading to a decrease in efficiency and stability over time. BEs tend to have shorter operational lifetimes compared to red and green emitters. This is partly due to the higher energy involved in blue light emission, leading to more stress on the materials and potentially faster degradation.

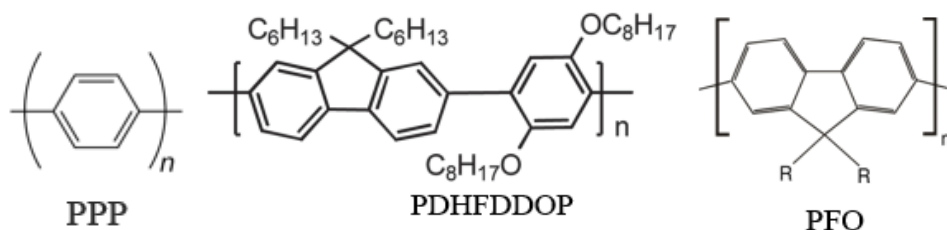


Figure 1.3. Chemical structures of some blue polymer emitters, poly-(para-phenylene) (PPP), poly(9,9-dihexylfluorene-alt-co2,5-didecyloxy-para-phenylene) (PDHFDDOP), polyfluorene (PFO), respectively.

Efficiently emitting deep blue light in OLEDs presents various challenges, such as limited availability of suitable emitters, low photoluminescence quantum yields, stability issues, and difficulties in achieving narrow spectral width and high color purity. Within the literature, the challenges are being addressed via material design, device engineering, and fabrication process improvements to enhance the performance of deep blue-emitting OLEDs for applications such as displays and lighting.

1.2. Aim of The Thesis

The aim of this thesis is to obtain color purity and stability by utilizing POSS group ended Polyfluorene (BE) in a solution processed single layer blue OLEDs. Coating conditions that have been thoroughly examined further contributes to device performance improvement. This method includes using the polyfluorene polymer and the perylene diimide small molecules dopants and the optimization of the film morphology to improve charge transport and emission efficiency. Furthermore, this study investigates Förster-type energy transfer (FRET) using polyfluorene as the donor and perylene diimide as the acceptor dopant to enhance light emission with efficient energy transfer. The intermolecular distance and orientation of the molecules optimizes this process and ultimately improves the color quality and overall efficiency of the blue OLED. When fabricating single layer device structures, the energy levels are adjusted to reducing of exciton quenching. Coating with appropriate energy levels of PVK and PVK: mCP is designed to achieve balanced charge transport, which is critical to increasing of device efficiency. For this purpose, different coating conditions were studied with the ADS231BE and electroluminescence characteristics, photophysical and morphological properties of the devices were investigated.

1.3. Experimental

This section provides a detailed description of the materials used in the device production process, as well as the devices used to characterize device performance and determine the optical and morphological properties of thin films coated during production.

1.3.1. Materials

Indium tin oxide (ITO) coated glass substrates with a surface resistance of 4-10 Ω/sq are exploited as transparent anode and were purchased from LUMTEC. Hydrochloric acid [HCl(aq)] was purchased from TEKKIM, poly (3,4-ethylenedioxythiophene):poly(styrene sulfonate) (PEDOT:PSS, A14083) was from Heraeus Clevios, Poly[9,9-di-(2-ethylhexyl)-fluorenyl-2,7-diyl] – End-capped with

Polysilsesquioxane (POSS) (ADS231BE) was provided from American Dye Source. Poly (N-vinyl carbazole) (PVK), 1,3-Di(9H-carbazol-9-yl) benzene (mCP), 4,7-Diphenyl-1,10-phenanthroline (Bphen), aluminum (Al), chlorobenzene, isopropanol and acetone were from Sigma Aldrich. Orange-red emitting material of N, N'-bis(2-ethylhexyl) perylene-3,4,9,10- dicarboxylic diimide (PDI(2EH) ref) and PDI(2EH)-1 were sensitized and characterized by Dr. Erkan AKSOY in his PhD thesis (Aksoy 2020). Cesium Carbonate (Cs_2CO_3) was provided from Across Organics.

1.3.2. Instruments

ITO/glass substrate cleaning was processed by ISOLAB ultrasonic bath and CUTE FC-10046 Oxygen (O_2) plasma system. All solution process coating were coated via Laurell WS-400B-6NPP LITE spin coater in atmospheric conditions. Evaporation of thin films were performed by the use of a physical vapor deposition (PVD) instrument attached to a LC Technology Solution Inc. glove box system in Nitrogen (N_2) atmosphere. Coating thickness and rate were monitored by INFICON SCQ-310C deposition controller by using a 6 MHz crystal sensor and frequency meter together with quartz oscillator which allowed controlling rate by 0.1 \AA/s . The coatings of the organic materials coated in the air environment were made in the OPTOSENSE physical vapor deposition (PVD) device. The coating thickness and coating rates were checked using the SCIENS SI-TM508 deposition monitor. The power supply of the device is REBORN ZDF-5227 model device. The calibration curves of the materials (tooling factor) for the coating ratio (4.3.1) were determined. EL spectra and luminance–voltage–current density (L–V–J) curves were obtained using a Keithley 2400 programmable source measurement unit and calibrated Hamamatsu C9920-12 measurement system combined with an integrated sphere (inside diameter of 3.3 inch). The detector and the sphere were connected with 1.5 m fiber cable. Ultraviolet-visible (UV-Vis) absorption and photoluminescence (PL) measurements were performed by using Edinburgh Instruments FS5 Spectrofluorometer. Film thickness was achieved by Klatencor MicroXM-100 optical profilometer. Surface morphology analysis was specified with Bruker-MMSPM Nanoscope 8 Atomic Force Microscopy (AFM). Raman spectrum was measured by a home-built setup using 532 nm laser with 100mW power.

1.3.3. Fabrication of Devices

Organic light-emitting diodes (OLEDs) emit light when coated with layers of various organic materials, metals, and semiconductors using different thin-film coating techniques. Each layer has distinct electrical and optical properties. Thus, thin-film technology is crucial for the production of OLEDs.

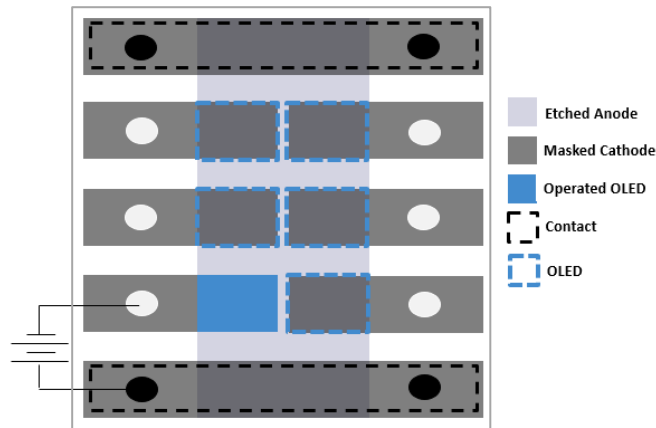


Figure 1.4. Top-side scheme of the fabricated devices.

Firstly, the ITO coated glass substrates purchased from LUMTEC were cut to a size of 2x2 cm with a diamond-tipped pencil. Secondly, the substrates were appropriately chemically etched with HCl(aq) and physically cleaned with detergent. Then, they were cleaned with detergent, water, deionize water, acetone and isopropyl alcohol, respectively for half an hour each, by using ultrasonic bath. After that, ITO coated glass substrates were dried with a N₂ gun then, 8 minutes O₂ plasma purification was applied to make the surface hydrophilic. For each device produced, the substrate preparation process is the same. After that, the organic layers (HIL, HTL and EML) were spin coated and the EIL and metal cathode were vacuum thermal evaporated using with shadow mask at 10⁻⁶ torr and the deposition rates of Cs₂CO₃ and Al were 0.2 Å/s and 2.0 Å/s, respectively. The OLED devices presented in this thesis have a basic device structure with 6 parallel devices and active areas of 7 mm² each as shown in Figure 1.4.

CHAPTER 2

THE FABRICATION OPTIMIZATION OF SOLUTION PROCESS POLYFLUORENE BASED BLUE OLEDs

In this chapter, the bare BE single-layer basic device structure has been used to generate blue OLEDs. For enhancement of the polyfluorene based device characteristic of blue OLED, different coating conditions were used and optimized of the most stable device fabrication process.

2.1. Importance of Polyfluorene Based Blue Organic Light Emitting Diodes

The first blue polyfluorene (PFO) based OLED was studied by Yoshino et al. in 1991 (Ohmori et al. 1991). Subsequently, Grice et al. conducted further research on PFO-based polymers (Grice et al. 1998). The device has been efficient and stable in its performance, with high color purity emission. Polyfluorene derivatives, with their combination of electroluminescent properties, tunable emission wavelengths, and solution processability, continue to be researched for advancements in various optoelectronic applications, including displays, lighting, sensors, and photovoltaics. They exhibit a conjugated structure with alternating single and double bonds along the polymer backbone. This structure enhances their electronic properties, making them useful in electronic devices. Also, they are known for their electroluminescent properties and emitting light when an electric current is applied. This makes them valuable for applications in OLEDs, where they can be used as emissive materials and the emission wavelength of PFO derivatives can be tuned by modifying the molecular structure. Many polyfluorene derivatives are soluble in common organic solvents, enabling solution processing methods such as spin coating or inkjet printing. For quality of thin film formation, they can form uniform and smooth films (W. Yang et al. 2003; Fan et al. 2007; L. Li et al. 2015).

The utilization of polyfluorenes in OLEDs faces a challenge due to the emergence of undesired green emission (Gong and Chang 2009; Kulkarni and Jenekhe 2003; Admassie et al. 2006; Xiao et al. 2003). This issue is attributed to either intermolecular interactions causing aggregate formation or the existence of emissive keto defects resulting from thermo- or electro-oxidative degradation of the PFO main chain. Consequently, the expected blue emission transforms into an undesirable blue-green emission in OLED applications. Numerous methods have been employed to minimize the formation of aggregation or keto defects in polyfluorenes. These approaches involve introducing bulky side chains, using cross-linked structures, enhancing oxidative stability in side groups or chain ends, and restricting chain mobility. A recent and innovative strategy involves integrating polyhedral oligomeric silsesquioxane (POSS) into the easily modifiable conjugated polymer. The initial investigation specifically focused on covalently attaching POSS to the chain ends of poly(9,9'-dioctylfluorene) (PFO), leading to an enhancement in the thermal stability of devices manufactured from these modified polymers (Gong and Chang 2009; Katz et al. 2000).

PFO-based OLEDs offer a host of advantages that contribute to their exceptional performance. One key strength lies in their chemical stability, ensuring durability and resistance to degradation over time. Thermal stability is another noteworthy property, allowing polyfluorene-based OLEDs to withstand varying temperatures without compromising functionality. The material exhibits blue emission, a crucial characteristic for achieving vibrant and high-quality color reproduction in displays. Furthermore, polyfluorene facilitates effective charge balance within the OLEDs, optimizing their overall performance. The ambipolar transport capability of polyfluorene ensures efficient movement of both positive and negative charges, enhancing the device's versatility and functionality. In summary, the combination of chemical and thermal stability, strong blue emission, charge balance, and ambipolar transport makes polyfluorene-based OLEDs stand out for their high device performance and reliability. Due to these advantages, studies on polyfluorene-based blue-light-emitting organic diodes, widely investigated in the literature, are summarized in Table 2.1.

In the scholarly literature, Hu et al. undertook the design and synthesis of a series of twisted blue-light-emitting derivatives of polyfluorenes, denoted as PNFSOs. Their efforts resulted in a notable enhancement of the maximum luminance, increasing from 2691 to 5481 cd/m². Furthermore, they observed a blue-shifted and narrowed electroluminescent spectrum, manifesting as a change in the CIE coordinates from (0.18,

0.18) to (0.16, 0.07), in comparison to both PFO and PNFSO5 (L. Hu, Liang, et al. 2019a). Additionally, the study explored derivatives of PNFSO10, identified as PFTAsSO10 and PFSO10T, wherein an elevation in thermal annealing temperature to 115°C yielded significantly improved electroluminescence performance in the blue-emitting polymers. This improvement was characterized by a maximum luminance of 14882 cd/m², a 3.6 V turn-on voltage, and a modified CIE coordinate of (0.16, 0.15) (L. Hu, Liang, et al. 2019a).

Lin et al. conducted the synthesis and characterization of a novel bipolar conjugated copolymer derived from PFO. Their findings indicated that the introduction of bipolar side chains into the polymer structure effectively hindered the intermolecular interaction of fluorene moieties. This modification facilitated a balanced charge injection and transport mechanism, leading to an enhancement in the emission of the polymer backbone. They reported the maximum luminance of 1189 cd/m² and the turn-on voltage at 4.2 V (Ying Lin et al. 2010). For enhanced blue electroluminescence stability, Feng et. al synthesized nano grid and they improved the stability and they reported the device based on PFO exhibits a turn-on voltage of 4.1 V, a maximum luminescence of 1237 cd/m², and a maximum EQE of 1.04% (Feng et al. 2019a).

To summarize the literature, a multi-faceted approach is required to increase the efficiency of blue OLEDs that use PFO as an emissive layer. Strategies include modifying the chemical structure of the polymer, introducing dopants, utilizing host-guest systems, and optimizing film morphology to improve charge transport and emission efficiency. Implementing tandem or multi-layer device structures, aligning energy levels, engineering interfaces, and applying controlled thermal annealing contribute to minimizing exciton quenching and improving overall device performance. Additionally, maintaining material purity is crucial to avoid impurities that may impact OLED efficiency negatively. These combined strategies aim to enhance brightness, stability, and overall efficiency in OLEDs utilizing conjugated polymer films.

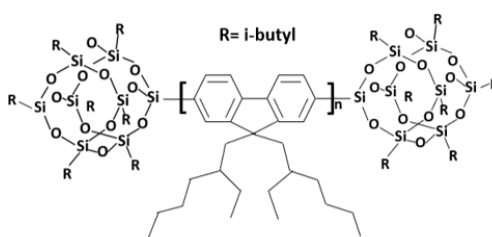
Table 2.1. Literature view of polyfluorene based blue organic light emitting diodes.

REF	Molecule	Device Structure	V _{turn-on} (V)	Lum (cd/m ²)	EQE (%)	CIE (x, y)
(Feng et al. 2019a)	PFO	ITO/PEDOT:PSS/PFO/TPBi/LiF/Al	4.1	1212	0.81	-
(L. Hu, Wu, et al. 2019)	PFO	ITO/PEDOT:PSS/EML/ Ba/Al	4.6	2691	-	0.18,0.18
	PNFSO2		4.3	3573	-	0.16,0.06
	PNFSO5		4.0	5481	-	0.16,0.07
	PNFSO10		4.0	3279	-	0.16,0.08
(Duarte et al. 2019a)	PFSO10TA2	ITO/PEDOT:PSS / EML/CsF/Al	3.6	14882	6.1	0.16,0.15
(Duarte et al. 2019b)	PFO	ITO/PEDOT:PSS/PVK/EML/Ca/Al	4.0	213	-	0.21,0.24
(Z. Huang et al. 2020)	PFO	ITO/PEDOT:PSS/EML/CsF/Al	3.4	1685	0.47	0.17,0.13
(Peng et al. 2020)	PFSO-2O	ITO/PEDOT:PSS/PVK/EML/Ba/ Al	2.9	19162	3.80	0.15,0.18
	PFSO-2BP		2.7	17650	5.46	0.15,0.16
	PFSO-BMD		2.7	24665	8.00	0.14,0.14
(Ying Lin et al. 2010)	PTHCF	ITO/PEDOT:PSS/ PTHCF:PBD/CsF/Ca/Al	8.9	4476	-	-
		ITO/PEDOT:PSS/ PTHCF/CsF/Ca/Al	4.2	1189	-	-
(Feng et al. 2019c)	PFO	ITO/PEDOT:PSS/PFO/TPBi/LiF/Al	4.1	1237	1.04	-
(Wan et al. 2021)	PFO	ITO/PEDOT:PSS/EML/Al	4.0	1245	-	-
	PFO:β phase		4.4	1583	-	-
(J. Xu et al. 2017)	PFO	ITO/ZnO/PEIE/TPBi/PF-FSO10/MoO ₃ /Al	5.8	-	7.1	0.15,0.15
		ITO/ZnO/PEIE/PF-FSO10/MoO ₃ /Al	6.0	-	5.9	0.15,0.15
(Shu et al. 2003)	PF-TPA-OXD	ITO/PEDOT:PSS/PF-TPA-OXD/Ca/Ag	12.0	4080	1.21	0.19, 0.14
(de Morais et al. 2023)	PFO	ITO/ PEDOT:PSS/PVK /PFO/ZnO/Ca/Al	4.0	432	-	0.15, 0.12
(Oide et al. 2023)	PFO	ITO/ PEDOT:PSS /PFO/AZO/Al	12.5	254.95	-	-

*Lum: maximum luminance, V_{Turn-on}: turn on voltage, EQE: external quantum efficiency, CIE: Commission Internationale de l'éclairage
 TPBi= 2,2',2''-(1,3,5-Benzinetriyl)-tris(1-phenyl-1-H-benzimidazole), CsF= Cesium fluoride, MoO₃= Molybdenum trioxide, ZnO= Zinc oxide, LiF=Lithium fluoride

2.2. Performances Polyfluorene Based and Perylene Diimides Doped Polyfluorene Based OLEDs

Single-layer blue-light-emitting OLEDs, employing an ITO/PEDOT:PSS/BE/Cs₂CO₃/Al device architecture, were fabricated on glass substrate through spin coating and vacuum thermal evaporation methodologies. The investigation encompasses a scrutiny of various coating environments, solvents, and annealing temperatures to ascertain the optimal parameters for blue fluorene-based OLEDs. Additionally, the study assesses the consequential effects of these conditions on the electrical and optical properties inherent in the devices.



ADS231BE

Figure 2.1. Chemical structure of purchased ADS231BE (“ADS231BE,” n.d.).

In the extant literature, it is documented that polyfluorene (PFO) manifests undesired emissions in the green spectral region attributable to keto defects (W. Yang et al. 2003; Gross et al. 2000; Duarte et al. 2019a). An approach to mitigating such defects involves their reduction by manipulating the annealing temperature (Katz et al. 2000). This study delves into diverse optimization conditions aimed at realizing the fabrication of pristine blue-light-emitting organic diodes while concurrently diminishing green emissions (Duarte et al. 2019c; Beigmohamadi et al. 2008; Kulkarni and Jenekhe 2003; Waddon and Coughlin 2003; Gong and Chang 2009; B. Liu, Zhang, et al. 2019; Jokinen et al. 2015).

2.3.1. Devices Characteristic

In our research group's prior investigations, examined the coating conditions of BE utilizing a cost-effective solution process method by Nuriye Demir (Demir 2014). The coating thicknesses were determined using PEDOT:PSS as a hole injection layer (HIL) (2000:1000 rpm, 2000rpm HIL, 1000rpm EML spin speed) (Yeşil 2017; Demir 2014). Regrettably, efforts to reduce emissions in the green region were complicated by the presence of keto defects in the electroluminescence (EL) curves extracted from the manufactured devices (Sevim et al. 2014; Diker, Yesil, and Varlikli 2019). A strategy documented in the literature is to address these keto defects by increasing the degree of crystallization by adjusting the annealing temperature. The importance of blue OLEDs lies in their crucial role in achieving an efficient and vibrant full-color spectrum. Maintaining color purity is essential to ensure that the emitted blue light remains distinct and well-defined, avoiding undesirable emission into neighboring wavelengths and preserving a nuanced contribution to the overall color palette.

Polymeric BEs, such as ADS231BE, are often considered due to their solubility and potential cost reduction. However, they face challenges related to broad electroluminescence, which can negatively affect color purity (Gong and Chang 2009; Duarte et al. 2019c). Notably, the morphological and electronic properties are profoundly influenced by the annealing temperature and the choice of solvent in this context (Gong and Chang 2009; Jokinen et al. 2015; S. Hu et al. 2020). Energy band diagram and side section view of fabricated devices are given in Figure 2.2.

PEDOT:PSS was filtered using a RC (regenerated cellulose) 0.45 μ m filter. The HIL was coated by using spin coater in air conditions (2000 rpm, 1 minute) and annealed at 150°C for 30 minutes. And BE (EML) was coated using in different solvents, annealing temperatures and different atmosphere conditions. Two different solutions of BE were prepared with toluene and chlorobenzene solvents and the coated films were annealed (1000 rpm, 1 min) at gradually increasing temperatures. Finally, as the EIL, Cs₂CO₃ (2.3 nm) and as the cathode, Al (100 nm) was coated using vacuum thermal evaporator at 10⁻⁶ torr and the deposition rates of Cs₂CO₃ and Al were 0.2 Å/s and 2.0 Å/s, respectively.

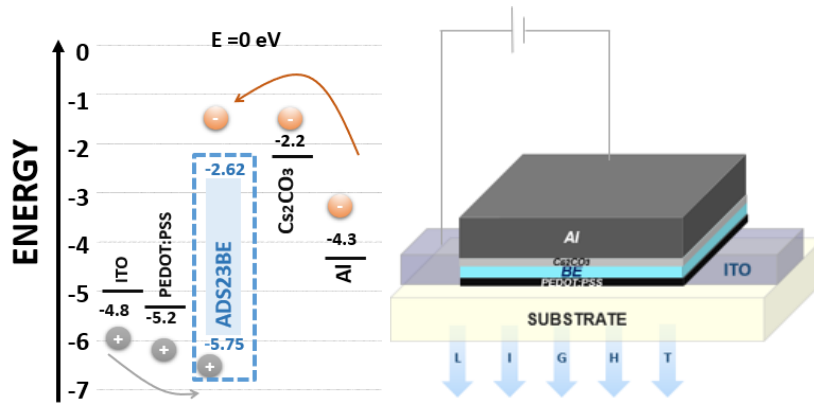


Figure 2.2. Energy band diagram and device structure of the fabricated devices with bare ADS231BE layer.

A typical OLED is fabricated by using BE as the emitter material and effect of annealing temperature on EL properties is investigated between 60°C and 150°C. In bare BE coated devices at atmospheric conditions, maximum efficiency values decreased with increasing annealing temperature, but efficiency losses decreased at high current density (A.1). The electroluminescence linewidth (or FWHM, nm) reduced drastically as the annealing temperature increased from 90°C to 120°C. These results indicate an improvement in the quality of blue radiation from the polymer. The obtained electrical and electro-optical characterization curves are shown in Figure 2.3 and the device yield values are given in Table 2.2. Due to the glassy transition temperature of the polymer at 74.11°C, the improvement observed between 90-120°C was investigated in detail in the fabricate of the other set of devices. Therefore, 75°C and 100°C were used as new annealing temperatures. Since no significant difference was observed between 120-150°C, annealing was not applied above 150°C. On the other hand, un-wanted green emission was decreased at same temperatures (Figure 2.3b).

In addition, BE layer coatings of these devices were also carried out in nitrogen (N₂) environment to prevent the possibility of keto defect formation due to dissolved oxygen in the atmosphere and solvent. Brightness, efficiency, color purity and electro stability were reported to be better when the coating atmosphere was N₂ and the coating conditions were optimized as N₂ atmosphere (A.2). In the device yields obtained, the yields of the devices produced in nitrogen environment were relatively higher and their stability increased. And, when the CIE coordinates were examined, improvements in color purity occurred. Thus, in parallel with the expectation, keto defect formation due to dissolved oxygen in the air was prevented (Katz et al. 2000).

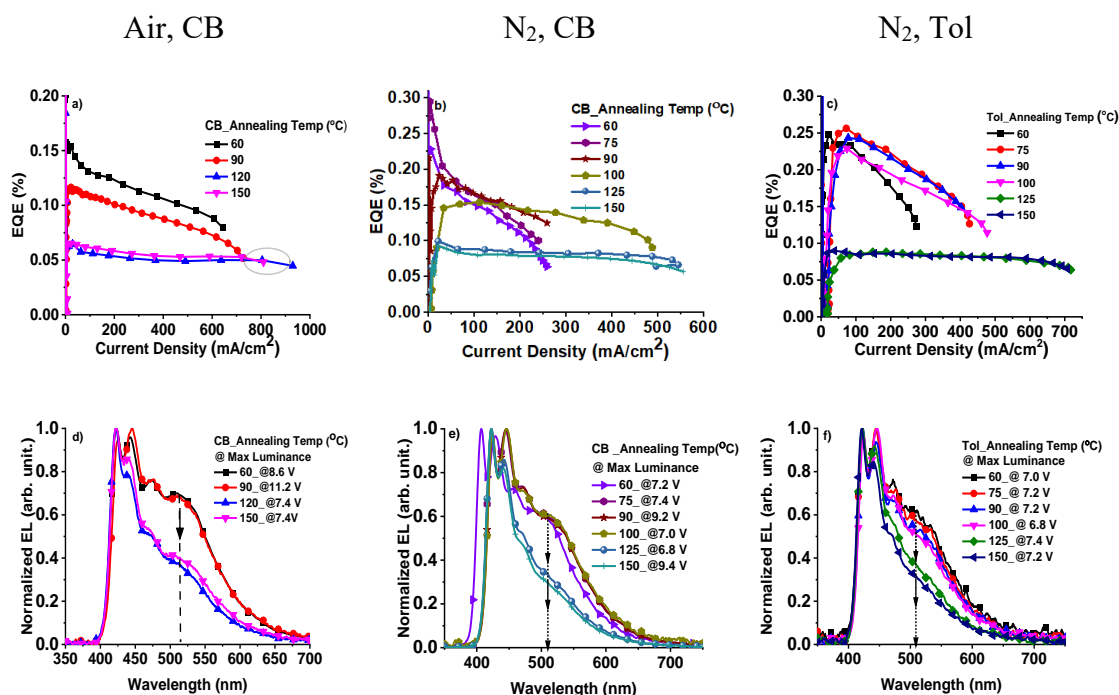


Figure 2.3. a, b, and c) external quantum efficiency vs current density and d, e and f) normalized electroluminescence vs wavelength at maximum luminescence characteristics of devices prepared by coating with chlorobenzene and toluene solvent and annealed at different temperatures in air and N₂ atmosphere, respectively.

Also, the effect of solvents to improve the light is also investigated in the literature. Different solvents directly affect the film structure. Solvent effect is important both for the formation of film morphology and for obtaining optoelectronic devices with high efficiency and stability (B. Liu, Zhang, et al. 2019).

Tol and CB are commonly used as solvents for polymers such as PFO. Tol is a non-polar solvent, whereas CB is polar and also has a higher dipole moment. Higher dipole moment can affect the solubility of the solution and the ability of the polymer to precipitate out of solution and form thin films. Solubility is important for the formation of homogeneous polymer solutions, which is critical for the uniform deposition of thin films, and PFO is generally soluble in non-polar solvents such as toluene. Therefore, the active layers of the third set of devices were reproduced in Tol solvent at a concentration of 10mg/mL, at the same annealing temperatures and nitrogen environment. The devices prepared with toluene solvent as the active layer showed no dramatic change in yields and color coordinates in the 60-100 °C range, but dramatic, EL half-wavelength (FWHM, nm) reduction occurred at 125-150 °C and color purity increased.

Table 2.2. Electroluminescence (EL) efficiencies of the devices annealed at gradually increased temperatures and prepared by coating with chlorobenzene and toluene solvents in air and N₂ atmosphere.

Atm	Sol.	Annealing Temp (°C)	Lum _{max} (cd/m ²)	Turn-on (V)	PE (lm/W)	CE (cd/A)	EQE (%)	CIE (x, y)	FWHM (nm)
Air	CB	60	1009	5.8	0.20	0.37	0.16	(0.22, 0.27)	129
		90	829	4.2	0.11	0.23	0.12	(0.22, 0.27)	126
		120	627	5.0	0.10	0.16	0.10	(0.20, 0.21)	53
		150	600	5.0	0.08	0.13	0.05	(0.20, 0.22)	56
N ₂	CB	60	428	5.2	0.24	0.43	0.23	(0.21, 0.25)	129
		75	480	5.4	0.26	0.46	0.30	(0.21, 0.24)	122
		90	565	5.0	0.16	0.31	0.18	(0.20, 0.23)	108
		100	848	3.8	0.15	0.27	0.15	(0.20, 0.23)	98
		125	547	4.6	0.10	0.16	0.10	(0.19, 0.18)	67
		150	472	4.6	0.19	0.14	0.28	(0.19, 0.17)	60
N ₂	TOL	60	680	4.4	0.29	0.49	0.25	(0.21, 0.26)	128
		75	1112	4.0	0.27	0.48	0.26	(0.21, 0.25)	127
		90	1105	4.0	0.25	0.47	0.24	(0.21, 0.25)	124
		100	1091	4.0	0.25	0.44	0.23	(0.21, 0.26)	126
		125	660	3.8	0.09	0.14	0.09	(0.19, 0.18)	61
		150	645	4.0	0.10	0.15	0.09	(0.19, 0.17)	49

*Lum_{max}: maximum luminance, Turn-on: turn on voltage, PE: power efficiency, CE: current efficiency, EQE: external quantum efficiency, FWHM: full width half maximum

Devices prepared using Tol demonstrated a reduced turn-on and an overall increase in luminescence and efficiency. As anticipated, devices with improved color purity in blue light have lower efficiency and luminance values. Nevertheless, the FWHM in Tol is 11 nm narrower despite being lower. Although CIE coordinates are the same ((0.19, 0.17) (Table 2.2) at 150°C annealing temperatures and in N₂ conditions, when we compared to CB and Tol solvents, FWHM values are measured as 60 nm and 49 nm, respectively.

Also, up to 100°C of annealing temperature OLEDs fabricated from Tol as solvent presented better efficiencies compared to the ones fabricated from CB. Irrespective of the solvent employed, the efficiency values decrease gradually. However, the stability and color purity of the devices exhibit an enhancement with an increase in the annealing temperature.

OLEDs fabricated with Tol as a solvent exhibit greater efficiency stability when compared to those fabricated with CB. Irrespective of the solvent employed, the degree of efficiency progressively falls as the temperature rises. Nonetheless, the stability and color purity of the devices exhibit a significant increase with higher annealing temperatures.

Table 2.3. x, y coordinate values of devices with BE active layer annealed at 125°C and 150°C varying with applied voltage.

Annealing Temp (°C)	Chlorobenzene	Toluene
125		
150		

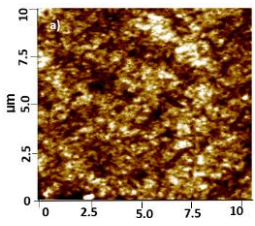
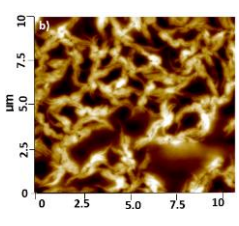
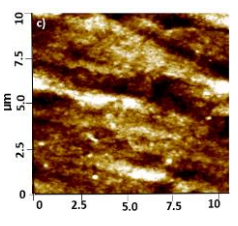
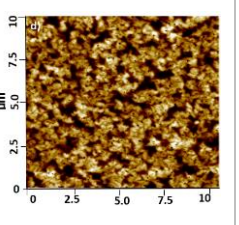
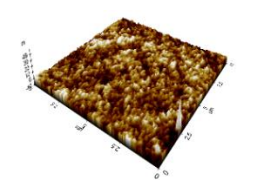
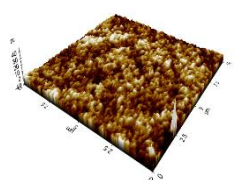
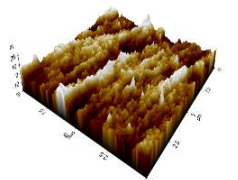
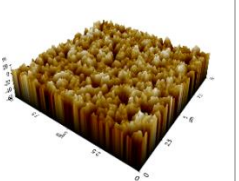
As the glassy transition temperature (74.11 °C) approaches, the anticipated outcome is an increase in luminescence alongside a decrease in the turn-on voltage. The device exhibiting the greatest luminescence values was found in Tol solvent, resulting in the 4.4 V reduction in turn-on voltage, an increase of the maximum luminance by 1112 cd/m² (@7.2 V), and the rise in the current efficiency by 0.48%. Additionally, CIE coordinates were measured and found to be (0.21, 0.25) and (0.19, 0.17) for the devices annealed at temperatures of 60°C and 150°C (Table 2.2, Figure 2.3, A.3 and A.4), respectively.

Stability with applied voltage is a major issue that needs to be addressed urgently, especially for the polymer diodes. Furthermore, the Table 2.2 provides the x and y coordinates of the produced devices that vary with the applied voltage. Although the coordinate values at maximum EL are identical in both solvents at comparable temperatures, the Δxy , in terms of the applied voltage, provides insight into the stability of the device color, i.e., how much less the voltage change affects the color. It is evident that the coordinates of the devices produced in toluene solvent at 150 °C remain almost unaffected by the applied voltage. As shown in Table 2.3d, the device with the best color stability versus applied voltage was found in Tol at 150 °C.

2.3.2. Morphology Analysis

The figures depicting the samples that were prepared via spin coating on mica at 2000 rpm according to the coating conditions of the initial devices are summarized in Table 2.4. Upon examining their surface topography, morphological variations were observed in the samples annealed at low and high temperatures in both solvents. On the surfaces annealed at 150 °C, there are clusters of crystalline images, which are larger than 2 μm in chlorobenzene solvent and approximately 1 μm in toluene solvent under nitrogen atmosphere. The surface is found to be more homogeneous when using toluene solvent. The average roughness in chlorobenzene and toluene solvents are 13.771 nm and 6.908 nm, at 150 °C respectively. At 75 °C, the average surface roughness for CB and Tol solvents are 1.283 nm and 2.903 nm respectively (Table 2.4). The effect of annealing temperature on morphology was clearly in evidence (Z. Huang et al. 2020).

Table 2.4. AFM images were obtained of BE films spin-cast at 2000 rpm on mica substrates using CB and Tol solvents at temperatures of 75°C and 150°C.

	CB		Tol	
°C	75	150	75	150
2D				
3D				
Ra (nm)	1.283	13.771	2.903	6.908

The BE backbones in the films showed a π - π stacking and occurred typical random grains in the high temperature. The grain size is bigger in CB, because of the solvent polarity. It is less polar than toluene so that, the physical stacking is bigger.

In summary, as a result of increased annealing temperature, undesired green emission increases have been minimized. Maximum color purity and stability have been

achieved in devices annealed at 150 °C. Also, morphology of BE given in Table 2.4, known from the literature, changing with temperature and solvent has been measured. And the topographic images show an interconnected network morphology reminiscent of aggregation at the highest annealing temperature independent from solvent in AFM measurement (Gong and Chang 2009; Katz et al. 2000).

2.3.3. Photophysical Analysis

Figure 2.4 represents the photoluminescence (PL) spectra of thin films excited at the excitation wavelength obtained. The optical properties of the polymer thin film were determined by spin-casting the solution on a mica substrate. The absorption and PL curves of the BE polymer are provided, with a maximum absorption wavelength of BE ($\lambda_{\text{abs max}}$) at 380 nm. Excitation at this wavelength results in $\lambda_{\text{emis max}}$ at 421 nm, accompanied by two shoulders at 443 and 543 nm.

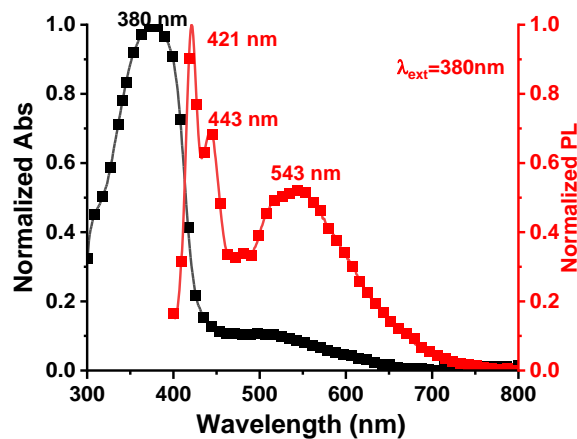


Figure 2.4. Photoluminescence and Absorption spectrums of BE active layers at 380 nm excitation wavelength thin film spectra.

CHAPTER 3

DEVICE PERFORMANCE OF POLYFLUORENE BASED AND PERYLENE DIIMIDE DOPED POLYFLUORENE BASED BLUE OLEDs

In this chapter, fabricated device characteristics was studied on perylene diimides (PDIs) doped PFO-POSS based and bare PFO-POSS based EMLs. In section 3.1, annealing temperatures were optimized and the analysis of fabricated OLEDs was discussed. Subsequently, OLEDs were studied on different HTLs in the specified conditions of EML and their optical, morphological and electronic properties of devices were analyzed, in ongoing sections.

The primary colors blue and orange, or the complementary colors red, green, and blue (RGB), are mostly used to create white light. Expanding emission spectra is an advantage of doping small molecule fractions of orange-red light-emitting photodynamic dyes (PDIs) into blue light-emitting polymeric materials (Ban et al. 2016; Schols 2011; Ju, Yoon, and Kim 2020; Sasabe and Kido 2013). It is challenging to obtain a high CRI and an efficient deep blue color in CIE coordinates when using primary colors, which are frequently used in phosphorescent and organic fluorophores. Subsequently, PDI(2EH)-ref and PDI(2EH)-1 (Figure 3.1) were doped in BE. Hence, it is aimed to increase the device efficiency using by PDIs fluorescent emission, which is a small molecule.

Currently in the lighting industry, white light is achieved by applying an orange-red coating to blue LEDs, with blue light exciting the orange-red light through photoluminescence, ultimately resulting in white light. The molecule responsible for emitting blue light, BE, is a polyfluorene derivative containing a POSS group, classified as a polycyclic aromatic hydrocarbon. This molecule possesses high solubility in both solution and film phases and can produce saturated blue light with a substantial fluorescence quantum yield. To enhance the thermal stability of fluorene and its resistance to oxidation, POSS groups have been affixed. As a result, π - π interaction of the molecule is also diminished. Both PFO-POSS as conjugated polymer and PDIs as small molecules have been employed as the core components of the EML to produce high-performance solution-processed OLEDs. It is predicted that PDIs will prevent physical

stacking by entering between decoupled polymer chains (L. Yang et al. 2019; H. S. Zhang et al. 2022). In the realm of PFO-based devices, host-guest systems are commonly developed to enhance the inherent optical-electronic properties of PFO.

The aim of this study is to enhance device properties by utilizing energy transfer through the decoupling of n-type chromophores from polymers of p-type behavior (Lu, Wang, and Pei 2021; J. Liu et al. 2018). In PFO-based OLEDs doped with PDIs, Förster-type energy transfer plays a pivotal role for non-radiative energy transfer. Here, PFO acts as the donor, while PDIs serves as the acceptor dopant within the OLED's emissive layer. This energy transfer mechanism is achieved through Förster resonance energy transfer (FRET), where the excited state energy of PFO is efficiently transferred non-radiatively to PDI (Abbel et al. 2009; Campbell et al. 2001). To optimize this process, factors such as dopant concentration, intermolecular distance, and molecular orientation are carefully controlled. The successful FRET enhances light emission, thereby improving the color quality and overall efficiency of the OLED (Dayneko et al. 2020; 2021).

In certain studies in the relevant literature, devices produced with perylene-doped ADS231BE active layers coated on PVK and PVK:mCP (3:1) layers, which exhibit different hole transport mobility, have achieved higher efficiency and brightness values compared to other HTL layers and host materials. The reason for this is believed to be the morphological interaction between HTL and EML, and it is thought that the interaction of PDIs with ADS231BE alters the surface topography (Pan et al. 2017).

3.1. Importance of Polyfluorene Based Perylene Diimide Doped Blue Organic Light Emitting Diodes

ADS231BE (BE) is a derivative of PFO with a POSS end group, a commercial material. And it suffers from high efficiency when emitting deep blue light. To improve the characteristics of the device such as spectral width that is narrow, high color purity and external quantum efficiency (EQE), the optimal coating conditions are optimized and n-type small molecule chromophores are doped within the p-type BE.

The variation in the electronic, optical, and film morphological properties of the device has a significant impact on changes in the physical structure or conformation of the molecule. Fluorene derivatives of the BE type undergo conformational modifications in response to specific annealing temperatures, solvents, or other external forces that can

induce physical changes (Fan et al. 2007; Tasch et al. 1997; Y. Xu et al. 2005). In the literature, various methods have been reported for inducing beta conformational states in BE-type conjugated polymers by exposing them to external forces, such as solvent and thermal-mediated techniques, both in the solution phase and in thin film structures produced at the glass transition temperature, exhibiting distinct morphological structures (Weinfurtner et al. 2000; Ban et al. 2016).

3.1.1. Perylene diimide based OLEDs

PDI is a class of organic compounds that has been studied for its interesting electronic and optical properties. PDI derivatives are commonly used in various electronic devices, including OLEDs. They are electron-accepting molecules due to their strong electron-withdrawing nature. The derivatives often exhibit high electron mobility, making them effective in transporting electrons within the device structure. PDIs are known for their planar and stable molecular structure. This stability contributes to the long-term performance and operational stability of OLED devices. PDIs have well-defined absorption and emission spectra. Their emission can be tuned by modifying the molecular structure. Some of them are soluble in common organic solvents, facilitating their processing into thin films for use in OLEDs (Cormier and Gregg 1997; Chen et al. 1998).

PDIs can serve as host materials in OLEDs, particularly in the emissive layer. By incorporating suitable dopants, they can contribute to light emission in specific colors. Due to their high electron mobility, they can enhance charge transport properties in OLEDs, leading to improved device efficiency. PDIs can be chemically modified to tune their absorption and emission properties. This allows for the design of OLEDs with specific colors and emission characteristics. Some PDIs are amenable to solution processing techniques, such as spin-coating, making them suitable for use in the fabrication of OLEDs. Some PDI derivatives can be processed from solution, which is advantageous for fabrication techniques such as spin-coating. Solution processing allows for the deposition of thin films, a key requirement in OLED device fabrication. Researchers continue to explore new PDI derivatives and optimize their use in OLEDs to enhance device performance, efficiency, and color quality (Bharathan and Yang 1998; Uoyama et al. 2012; Brown et al. 1999).

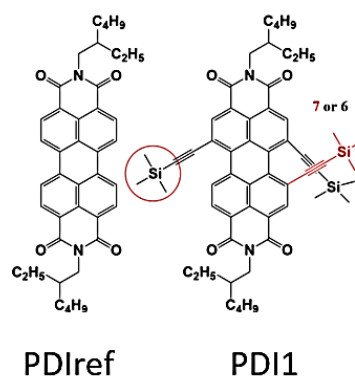


Figure 3.1. Chemical structure of synthesized perylene derivatives PDI(2EH)-ref and PDI(2EH)-1 by Erkan Aksoy (Aksoy 2020).

PDI derivatives offer several advantageous properties, they also come with certain limitations and disadvantages. Besides all these positive properties, PDIs are typically associated with red or orange emissions, which may limit their application in white light emission. Expanding the range of colors, particularly in the blue region, can be difficult using only PDI derivatives. The synthesis of certain PDI derivatives can be complex, which may pose challenges in terms of scalability and cost-effectiveness for large-scale production in commercial applications. Some PDI derivatives may have limitations in terms of their compatibility with certain device processing techniques. For instance, issues related to solubility or film formation may impact the production process. Although PDI derivatives generally exhibit high electron mobility, their properties can vary depending on the specific molecular structure. Certain derivatives may have lower electron mobility, which can affect their effectiveness as electron transport materials in specific OLED configurations. The synthesis and purification of PDI derivatives can involve multiple steps, which may contribute to higher production costs compared to other organic materials used in OLEDs (Chang et al. 2017; B. Zhang et al. 2017; Yuze Lin and Zhan 2015).

Furthermore, PDI molecules typically contain aromatic rings, and one of the primary driving forces for aggregation is π - π stacking. This interaction involves the stacking of aromatic rings on adjacent molecules, leading to the formation of aggregates. π - π stacking is particularly strong in planar aromatic structures like those found in PDI derivatives (Figure 3.1). Van der Waals forces as well, including London dispersion forces, play a significant role in the aggregation of PDI molecules. These forces arise from the temporary fluctuations in electron distribution within molecules and contribute

to the attractive forces between adjacent PDI molecules. Moreover, the hydrophobic nature of PDI derivatives can lead to aggregation in nonpolar solvents. Hydrophobic interactions between the nonpolar portions of PDI molecules drive the assembly of aggregates to minimize exposure to the surrounding polar solvent. Also, higher concentrations of PDI molecules in a solution or thin film can increase the likelihood of aggregation. At elevated concentrations, the chances of molecular collisions leading to π - π stacking and other attractive interactions are higher. And the choice of solvent can influence the degree of aggregation. Some solvents may promote aggregation due to their ability to facilitate π - π stacking, while others may help disperse PDI molecules. The type and position of substituents on the PDI core can influence the density of aggregation. Bulky or polar substituents may disrupt aggregation by introducing steric hindrance or altering the intermolecular forces (Zong et al. 2018; Matussek et al. 2018; Icil 1998; Chang et al. 2017; B. Zhang et al. 2017). For all these reasons, small molecule PDIs can increase the charge transmission with host-guest system and can reduce the charge transmission in the device by doped trace amounts to the polymers.

3.1.2. Device Characteristics

PDI doped BE and BE active layer devices produced by forming thinner films by coating at 3000 rpm were annealed at 75°C, which is just above the glass transition temperature, and at 150°C, which has shown more stable yields in previous studies. The active layers were reproduced in toluene solvent at a concentration of 10mg/mL, with PDIref and PDI1 doping ratios of 0.1 wt.%, annealing temperatures of 75°C and 150°C and in N₂ environment. And HIL and EML were coated in 3000rpm per minute. The device structure is ITO/PEDOT:PSS/BE:PDIref (or PDI1)/Cs₂CO₃/Al and the energy band diagram and device architecture are given in Figure 3.2.

The devices were reproduced by a different thickness of HTL and EML and the active layers were reproduced. When considering the devices with BE active layer, the spin coating rate of PEDOT:PSS and BE was increased in contrary to the previous study. Improvements in the efficiency values at 150°C were observed with different film thicknesses. Although PDIref doping increases the yield at 75°C, a similar situation is not observed at 150°C. PDI1 doping resulted in an improvement of the devices. The EL

characteristics of BE and PDI doped BE devices are summarized in Figure 3.3 and Table 3.1.

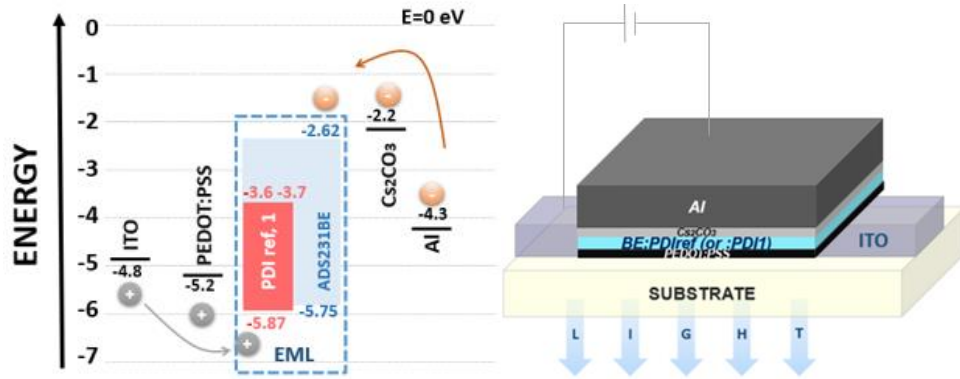


Figure 3.2. Energy band diagram and device structure of the fabricated devices with PDIs doped emissive layers.

PDI doping appears to enhance the yields by roughly 20%, and concomitantly, there is a noteworthy reduction in FWHM at 75°C. The table indicates an increase in turn-on voltage and a corresponding decrease in luminance values. At 150°C, the efficiency values are nearly doubled for the BE active layer device. The balance of electrons and holes is important for light generation in OLEDs. When the charges are in balance, the exciton recombination increases which leads to an indirect escalation in efficiency values and luminance. It is anticipated that the device architecture will incorporate HTL in upcoming studies to enhance the hole transition between the HIL and the EML, thereby reducing exciton quenching.

PDI-doped BE and BE active-layer devices, which were produced with a thinner coating of 3000 rpm, were annealed at 75°C, just above the glass transition temperature, and at 150°C, which has shown more stable yields in previous studies. PDI doping demonstrated a 20% increase in yields and concomitantly resulted in a significant reduction in FWHM at 75°C. The reduction of unwanted green emission is shown in the Figure 3.3b and Figure 3.3f of PFO (Bai et al. 2017; Kulkarni and Jenekhe 2003). A rise in turn-on occurred, along with a decrease in luminosity values, as summarized in the Table 3.1.

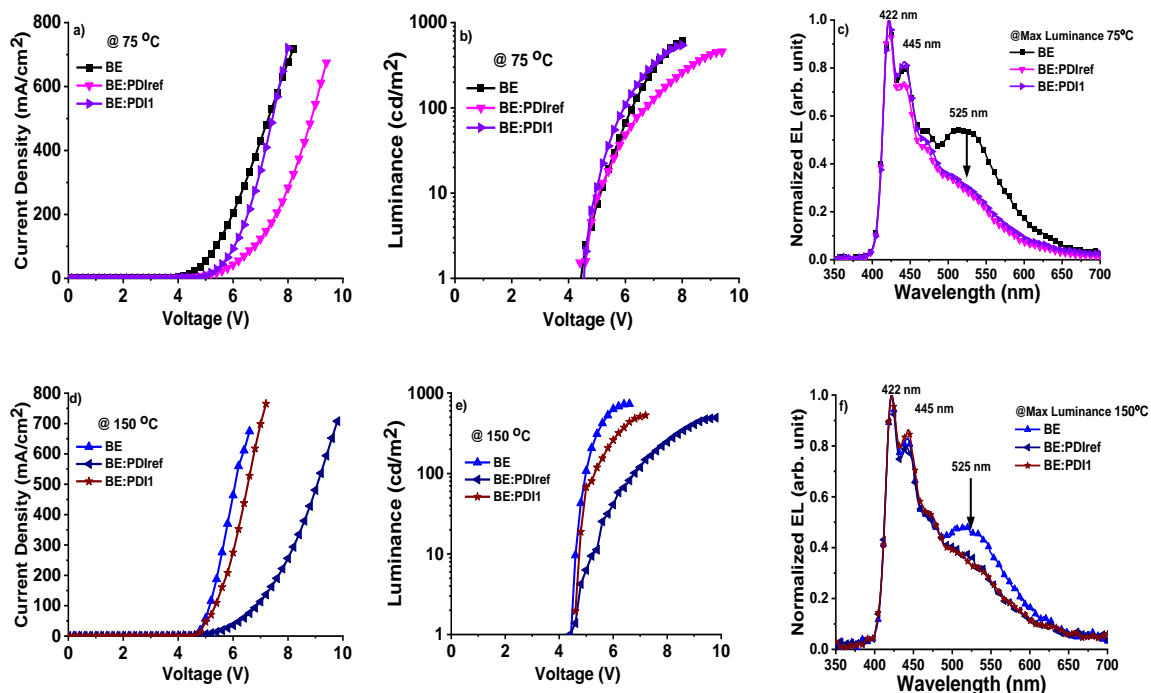


Figure 3.3. a) and d) current density, b) and e) luminance vs applied voltage and c) and f) normalized electroluminescence vs wavelength at maximum luminescence characteristics of devices prepared by BE and PDIs doped BE emissive layer. a, b, c at 75°C and d, e, f at 150°C, respectively.

For device characteristic of the bare BE emissive layer, when compared with 1000 rpm vs 3000 rpm film thickness, the color coordinates and FWHM values approximately equal but the efficiencies and luminance were decreased with reducing film thickness in Table 2.2 and Table 3.1, respectively. ADS231BE is a conjugated polymer and has strong π - π interactions which contribute to the delocalization of π -electrons along the polymer backbone. This extended conjugation enhances the electronic conductivity of the polymer with thin film thickness.

As the film thickness decreased, the EL properties were obtained between bare BE EML devices, the maximum luminance increased from 645 to 732 cd/m^2 , the current efficiency improvement from 0.15 to 0.23 cd/A . Also, turn-on voltage, CIE coordinate and FWHM distance do not change in thinner film thickness.

The balance of electrons and holes is important for light generation in OLEDs. When the charges are in balance, the exciton recombination increases which leads to an indirect escalation in efficiency values and luminance. It is anticipated that the device architecture will incorporate HTL in upcoming studies to enhance the hole transition between the HIL and the emitter layer, thereby reducing exciton quenching.

Table 3.1. Electroluminescence efficiencies of the BE and PDIs doped BE devices.

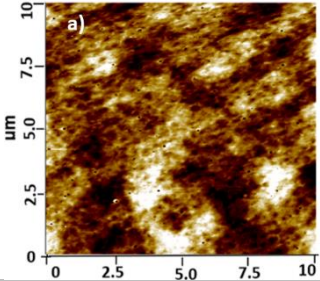
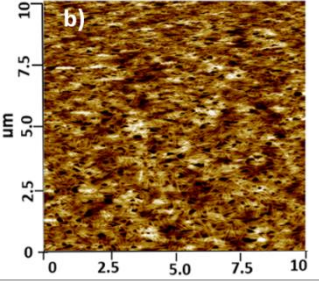
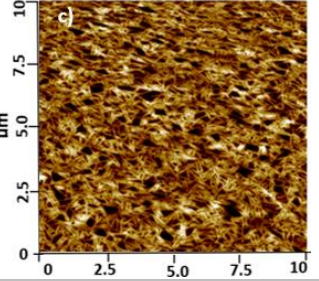
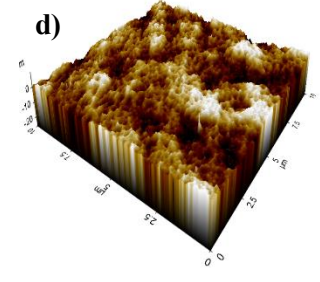
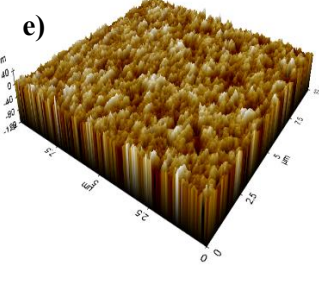
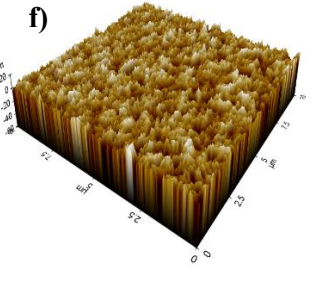
Annealing Temp (°C)	Emissive Layer	Lum _{max} (cd/m ²)	Turn-on (V)	PE (lm/W)	CE (cd/A)	EQE (%)	CIE (x, y)	FWHM (nm)
75	BE	613	4.0	0.04	0.09	0.05	(0.21, 0.25)	127
	BE:PDlref	457	4.4	0.06	0.11	0.08	(0.19, 0.19)	61
	BE:PDlI	543	4.6	0.08	0.13	0.09	(0.20, 0.19)	59
150	BE	732	4.0	0.15	0.23	0.13	(0.19, 0.17)	49
	BE:PDlref	494	4.4	0.07	0.13	0.08	(0.20, 0.21)	51
	BE:PDlI	528	4.2	0.12	0.14	0.08	(0.20, 0.20)	53

Exciton quenching refers to non-radiative processes that can deactivate excitons before they have a chance to emit light. By reducing exciton quenching, the efficiency of the OLED can be further enhanced. Therefore, the proposed use of the HTL in the device architecture is seen as a strategy to improve the overall performance of OLEDs by promoting a more efficient and balanced recombination of electrons and holes, ultimately leading to higher efficiency values and luminance. For these reasons, we utilized HTL materials in the OLED structure in later studies and optimized the essential conditions.

3.1.3. Morphological Analysis

The AFM images of bare BE and PDIs doped BE films are shown in Table 3.2. The AFM samples were prepared on mica substrate and they were spin-coated 3000 rpm and thermally annealed at 150 °C. As seen in the Table 3.2a and b the bare PFO-POSS backbones in the film showed a π - π stacking (L. Hu, Liang, et al. 2019b; Pal, Gedda, and Goswami 2022; Abbel et al. 2018; Lova et al. 2017a). The thickness of the film coated at 1000 rpm is much greater than that of the film coated at 3000 rpm and, as can be seen from the morphologies (Table 2.4 vs Table 3.2a), stacking is more intense in the thicker film. As expected, the root mean square values are 6.91 nm for thick film and 1.28 nm for thin film.

Table 3.2. AFM images of a) ADS231BE b) PDIref doped 0.1 %wt. BE and c) PDI1 doped 0.1 %wt. BE thin films spin casting in mica substrate at 3000rpm-min with 10mg/mL toluene and annealed at 150°C. And d, e, f are 3D images of their, respectively.

	BE	BE:PDIref	BE:PDI1
2D			
3D			
Ra	1.275 nm	9.322 nm	5.033 nm

*Ra: Roughness average of the films of 10 μ m*10 μ m.

On the other hand, when the PDIs are doped within the π -conjugated polyfluorene, the typical small random grains are changed and microneedle structures have been observed. Typically, the formation of microneedles involves materials with certain properties or responses to specific conditions that lead to their self-assembly into needle-like structures and this has been reported for PDIs (Pal, Gedda, and Goswami 2022; Görl et al. 2015). Also, in Table 3.2d the 3D images of BE are seen like tightly stacked cylinders. Then, when PDIS is doped, it looks like these cylinders are thinner, in Table 3.2e and f. This suggests that PDIs cause an aggregation in polymer chains (Lova et al. 2017b; Y. Li, Zhang, and Liu 2021).

Analytical methods were used to clarify the changes in morphology and aggregation that occurred. Photoluminescence measurements were used provide information about the molecular uniformity and structural characteristics of the thin films. Additionally, the Raman measurements were used provide information about the vibrational modes of molecules, offering insights into the molecular arrangement, bonding state, and structural characteristics of the film.

3.1.4. Photophysical Analysis

For investigation of the effect of steric hindrance on the thermal stability of BE, which ended with POSS group, AFM was used to study variation in the detailed film morphology before and after doping PDI derivatives as shown in Table 3.2. Uniform films were deposited by spin-casting from toluene solutions; the films showed a roughness of 1.28, 9.32, 5.03 nm for fabricated devices. For understanding the occurring morphology, the photophysical analysis were studied. The samples were prepared on glass substrate as thin film.

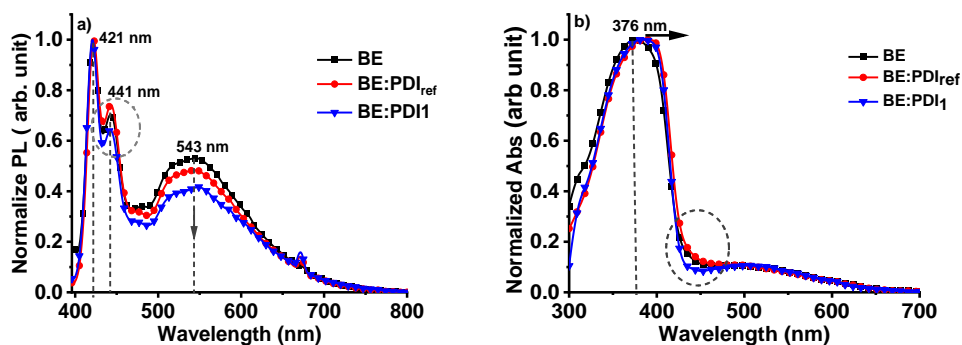


Figure 3.4. a) Photoluminescence spectrum and b) absorption spectrum of solid-state thin films of active layers excited at 380 nm.

Figure 3.4 represents the PL spectra of thin films excited at the excitation wavelength obtained. The optical properties of the polymer thin film were determined. The absorption and PL curves of the BE polymer are given in Figure 3.4. The maximum absorption wavelength of BE ($\lambda_{\text{abs max}}$) 376 nm, and with excitation at this wavelength it is $\lambda_{\text{emis max}}$ 421 nm. $\lambda_{\text{emis max}}$ is accompanied by one shoulder at 443 and a broad peak at 543 nm. The absorption peak slightly shifted to red in the major peak at 376 nm. Also occurred a decreasing at 440nm in the absorption peak (T. Li et al. 2016).

In the solid state, it exhibits stable and strong blue emission between 421 and 441 nm, with a well-marked change in intensity, as shown in Figure 3.4a. The decrease of the peak intensity at 441 nm occurred and I_{421}/I_{441} changed (T. Li et al. 2016). The dramatic increase in the broad emission band around 540 nm indicates molecular chain differences in the PL spectrum. PL spectra were used to detect j-aggregation (Lova et al. 2017c) obtained from AFM images shown in Table 3.2, and the absorption wavelengths of PDI_{ref} and PDI₁ were expected to shift red in the film phase. The spectra of PDI-doped

thin films in this region were examined by stimulating the PDIs according to the wavelength detected in the previously determined film phase.

3.1.5. Raman Spectroscopy Analysis

Raman spectroscopy represents an influential analytical method in polymer research. Acquiring data related to molecular vibrations and rotational transitions within materials is essential for gaining insight into the structure, composition, and behavior of polymers. The wavenumber range of 100-1000 (movement of alkyl chain) gives the side chain movement and the wavenumber range of 1000-1600 (unit movement of fluorene) gives the main chain movement (B. Liu, Bai, et al. 2019).

The Raman spectra showed enhanced intensity and a soft shift of approximately 6 cm^{-1} from 1304 cm^{-1} to 1298 cm^{-1} for BE:PD_{Iref} as shown in Figure 3.5b, the main chain transition towards the chain geometry with more planarity; the enhancement of the peak intensity was attributed to C–C stretching modes between the phenylene rings and C–H in-plane bending modes. Importantly changing at 1250 cm^{-1} , which represents planarity of polymer chain geometry, was increased from (I_{BE}) 0.500 to 0.560 and 0.685 in $I_{BE:PD_{Iref}}$ and $I_{BE:PD_{II}}$, respectively. On the other hand, the intensity ratio at I_{1304}/I_{1343} of BE thin film, was obtained 1.275 and it was obtained 1.433 and 1.191 for BE:PD_{Iref} and BE:PD_{II}, respectively. So that, changes in the main chain conformation occurred because the peak intensity from 1100 cm^{-1} to 1400 cm^{-1} increased compared to that of BE thin films, which forming the same pattern (Table 2.4) (B. Liu, Bai, et al. 2019). A soft shift of 4 cm^{-1} at 1600 cm^{-1} , which further confirmed the quasi-planar conformation of the BE chain in the spin casting film. As shown in Figure 3.5a, which represents C=C stretching motions, indicates a more planar chain conformation and this situation makes us think that the transformation from α conformation to β conformation, as confirmed by absorption, PL and Raman spectroscopy. The bending angle of PFO in α conformation is 135° while it is 165° in β conformation (Bai et al. 2017; T. Li et al. 2016; B. Liu, Zhang, et al. 2019).

When J-aggregation occurs in a polymer system, it can lead to changes in how the polymer chains are aligned or packed together (Yamagata and Spano 2014). The J-aggregation can lead to changes in the conformation or packing arrangement of the polymer chains (Y. Di Liu et al. 2019). This can be inferred from the changes in the

Raman spectra (B. Liu, Bai, et al. 2019). The aggregates act as nucleation centers to promote the formation of β phase, which enhances the interaction of PFO-POSS chains and improves the planarity of PFO-POSS backbone, resulting in the formation of ordered aggregation (L. Huang et al. 2012).

When J-aggregation occurs in a polymer system, it can lead to changes in how the polymer chains are aligned or packed together. The J-aggregation can lead to changes in the conformation or packing arrangement of the polymer chains. This can be inferred from the changes in the Raman spectra (Spano and Silva 2014; Deng et al. 2014). The aggregates act as nucleation centers to promote the formation of β phase, which enhances the interaction of PFO chains and improves the planarity of PFO backbone, resulting in the formation of ordered aggregation (L. Huang et al. 2012; T. Li et al. 2016). This can affect the overall properties of the material, such as its optical properties, electronic behavior, or mechanical characteristics.

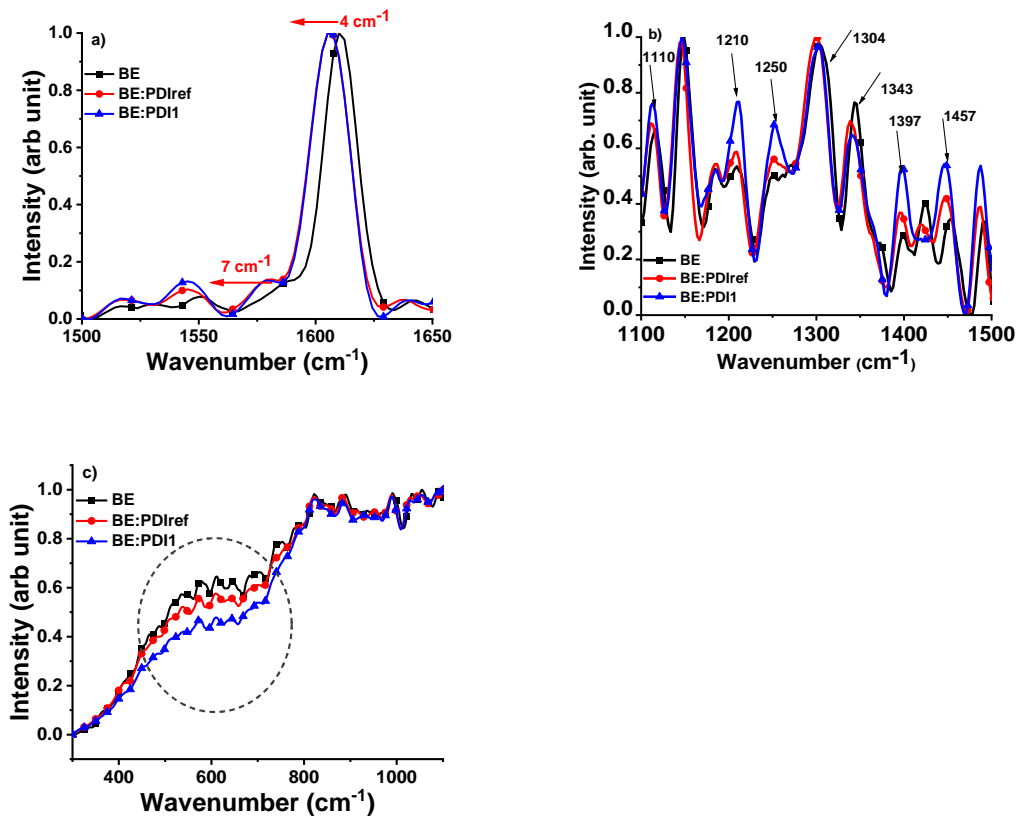


Figure 3.5. Solid state Raman spectra in the high wavenumber region between a) 1550-1650 cm^{-1} , b) 1100-1500 cm^{-1} and c) in the low wavenumber region 300-1100 cm^{-1} all active layer without HTL layers.

According to Kasha's theory, Frenkel excitons can couple in H-type or J-type aggregates, specifically in H-type coupling results in an optical transition that shows a blueshift with lower quantum yield (QY) compared to the monomer (Kasha, Rawls, and Ashraf El-Bayoumi 2009). Due to this reason, H-aggregates are not favored for applications in fluorescence. On the other hand, J-aggregates are expected to exhibit increased vibrational strength of the highest Frenkel exciton state, resulting in redshifted and narrower absorption and photoluminescence bands compared to the monomer (Tischler et al. 2005), as show in Figure 3.4.

As a result, parallel outcomes have been observed in morphological changes through both photoluminescence and Raman measurements. It is believed that polymer molecules form J-aggregates through head-to-tail assembly, and small molecules surround the resulting core. The formation of a shell around the core by the PDIs are thought to induce a β -conformational change in the molecular structure of the polymer. As the effects of PD_{Iref} on morphology, PL, and Raman were found to be the same as those of PD_{I1}, subsequent studies have been exclusively continued with PD_{Iref}.

3.2. Polyfluorene Based and Perylene Diimide Doped Polyfluorene Based OLEDs with HTLs

The high charge generation barrier of blue light-emitting materials due to their wide bandgap causes a charge imbalance in the active layer. For these reasons, the efficiency of devices for blue light generation is lower than green and red. In various studies, a hole transfer layer is employed to prevent any imbalances. The HTL in OLEDs serves a pivotal role by facilitating the efficient injection and mobility of positive charge carriers, or holes, from the anode to the emissive layer and it is designed to enhance hole injection, ensuring rapid movement of holes through the layer. Importantly, it exhibits good hole mobility while concurrently blocking the transport of electrons back to the anode, thereby maintaining charge balance within the device. This selective charge transport contributes significantly to the overall efficiency, luminance, and color accuracy of the OLED device. Additionally, the HTL provides a smooth interface on the anode, promoting uniform performance and device longevity. Typically composed of specialized organic materials, the HTL plays a critical role in optimizing OLED.

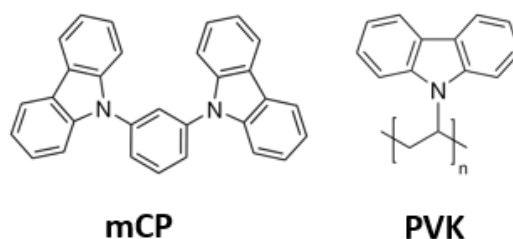


Figure 3.6. Chemical structure of 1,3-bis(carbazol-9-yl) benzene (mCP) and Poly(N-vinylcarbazole) (PVK)

PVK is a widely used HTL material in OLEDs. It exhibits high hole mobility, enabling efficient charge carrier transport. PVK's film-forming ability facilitates easy deposition as a thin, uniform layer, ensuring compatibility with organic layers and forming a stable interface. With good thermal stability and tunable energy levels through doping, PVK contributes to the prevention of electron leakage and supports reliable device operation. Its amorphous nature and commercial availability further make PVK a convenient choice for enhancing charge transport properties in various organic electronic applications. However, PVK faces challenges related to susceptibility to photoaging degradation, resulting in conformational rearrangements and chemical changes such as chain scission, oxidation, and cross-linking. These degradation processes lead to observable structural changes in photoluminescence spectra, which could affect the material's stability over the long term. Specific cross-linking reactions, especially at the carbazole units, have been identified as significant influencers in the degradation process. Therefore, applications requiring extended and stable performance mandate thorough consideration (Dayneko et al. 2021; Ostroverkhova 2016; L. Hu, Liang, et al. 2019c; Duarte et al. 2019d; Lova et al. 2017b, Bozkus, Aksoy, and Varlikli 2021).

Cost considerations are important for the scalability and commercial viability of OLED technology. The hole mobility of PVK is $2.5 \times 10^{-6} \text{ cm}^2/\text{V}\cdot\text{s}$. But, PVK electron mobility is comparatively lower. This can limit its effectiveness in facilitating the movement of electrons, which is essential for a balanced charge transport in OLEDs. PVK may have limited solubility in certain solvents, which can affect the ease of processing and manufacturing. Solubility is a crucial factor for solution processing techniques such as inkjet printing. PVK, like many organic materials, can be sensitive to environmental factors such as moisture and oxygen. This sensitivity can lead to device degradation over time. As another HTL material, mCP is known for its efficient hole transport capabilities. The hole mobility of mCP is $1.2 \times 10^{-4} \text{ cm}^2/\text{V}\cdot\text{s}$. It exhibits good thermal and

chemical stability, contributing to the overall stability of OLED devices. This is important for long-term performance and reliability. Also, it can be easily processed into thin films using techniques like spin-coating. mCP is often compatible with various organic emissive materials used in OLEDs. This compatibility is essential for achieving uniform and efficient charge transport within the device. PVK is relatively cost-effective compared to some other organic materials, contributing to its widespread use in OLED research and manufacturing. PVK has good hole transport properties, facilitating the efficient movement of holes from the anode to the emissive layer. This is crucial for the overall performance of the OLED device. PVK exhibits good thermal stability, allowing OLED devices to maintain their performance under varying temperature conditions. This stability is essential for the reliability and longevity of the devices. PVK can be easily processed into thin films, making it suitable for the fabrication of OLED devices using various deposition techniques, such as spin-coating or vapor deposition. PVK is often compatible with other organic materials used in OLED devices, allowing for the creation of well-organized and stable device structures.

The combination of PVK and mCP as a blend in an OLED serves a specific purpose, typically employed as HTL. The high thermal stability of mCP further supports stable device operation, especially in conditions where elevated temperatures might be encountered. Blending PVK and mCP allows for the optimization of charge injection, transport, and recombination in the OLED. The compatibility of these materials enables the creation of a homogeneous and well-functioning HTL, crucial for achieving improved device efficiency and stability (Bozkus, Aksoy, and Varlikli 2021) (Figure 3.6).

However, it's essential to consider the potential challenges associated with the blend, such as optimizing the concentration ratio of PVK and mCP to achieve the desired charge balance. Additionally, the long-term stability of the OLED device may be influenced by factors such as material compatibility and degradation over time. Careful consideration and optimization of the PVK and mCP blend are crucial for achieving the desired performance in OLED applications. In this study, the hole transport layers (HTL) used were PVK and PVK:mCP in a ratio of 3:1. Volkan Bozkus conducted a study of these HTL layers at TÜBİTAK as part of project number 119F031.

3.2.1. Devices Characteristic

The implementation of mCP has proven effective in achieving improved charge balance as a result of its high hole mobility. Additionally, it is anticipated that n-type perylene derivatives will enhance the electron-hole balance through augmentation of electron mobility. In the produced devices, PVK and PVK:mCP were formulated using a 10mg/mL chlorobenzene solvent. The PVK:mCP ratio of 3:1 was deduced by mass. The active layer, BE, BE:PDlref (kt 0.1%), and BE:PDI1 (kt 0.1%) were prepared with toluene solvent at a density of 10 mg/mL, for both HTLs. The energy band diagrams depicted in Figure 3.7 and the contents listed in Table 3.3. The HTL was subjected to spin coating at a speed of 3000 rpm and then annealed at 120 °C for a duration of 30 min. EML were spin coated at a speed of 3000 rpm and annealed at 150 °C. Vacuum thermal evaporation was used to coat Cs₂CO₃ 2.3 nm and Al 100 nm. Device architecture is ITO/PEDOT:PSS/PVK:mCP (or PVK)/EML/Cs₂CO₃/Al.

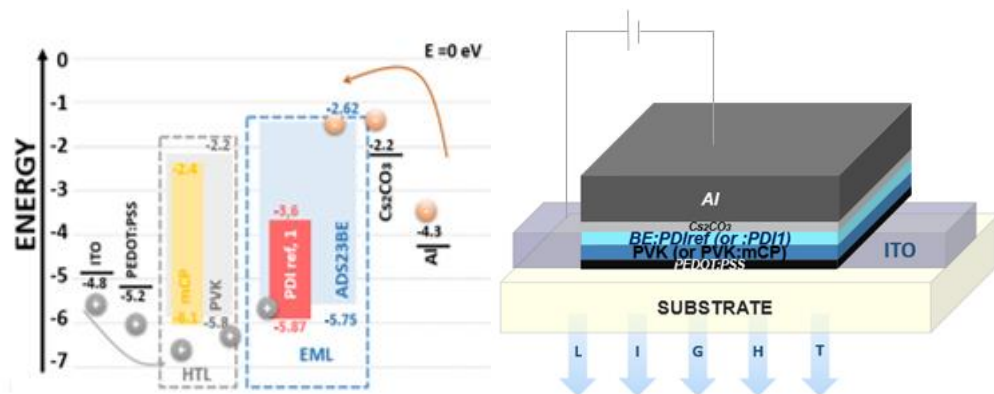


Figure 3.7. Energy band diagram and device architecture of the fabricated devices.

Table 3.3 shows the device efficiencies and luminance values, from which it is apparent that the effect of HTL can be clearly observed. The inclusion of PVK resulted in an increase in both device luminance and efficiency of approximately 500% (without HTL: 732 cd/m², 0.13% vs. with PVK: 3610 cd/m², 0.60), and was also responsible for an increase in FWHM. Furthermore, when PVK:mCP was present, there was six times increase in luminance, while efficiency values were enhanced by up to five times (732 cd/m², 0.13% vs 4412 cd/m², 0.57%, respectively) (Figure 3.8 and Table 3.3).

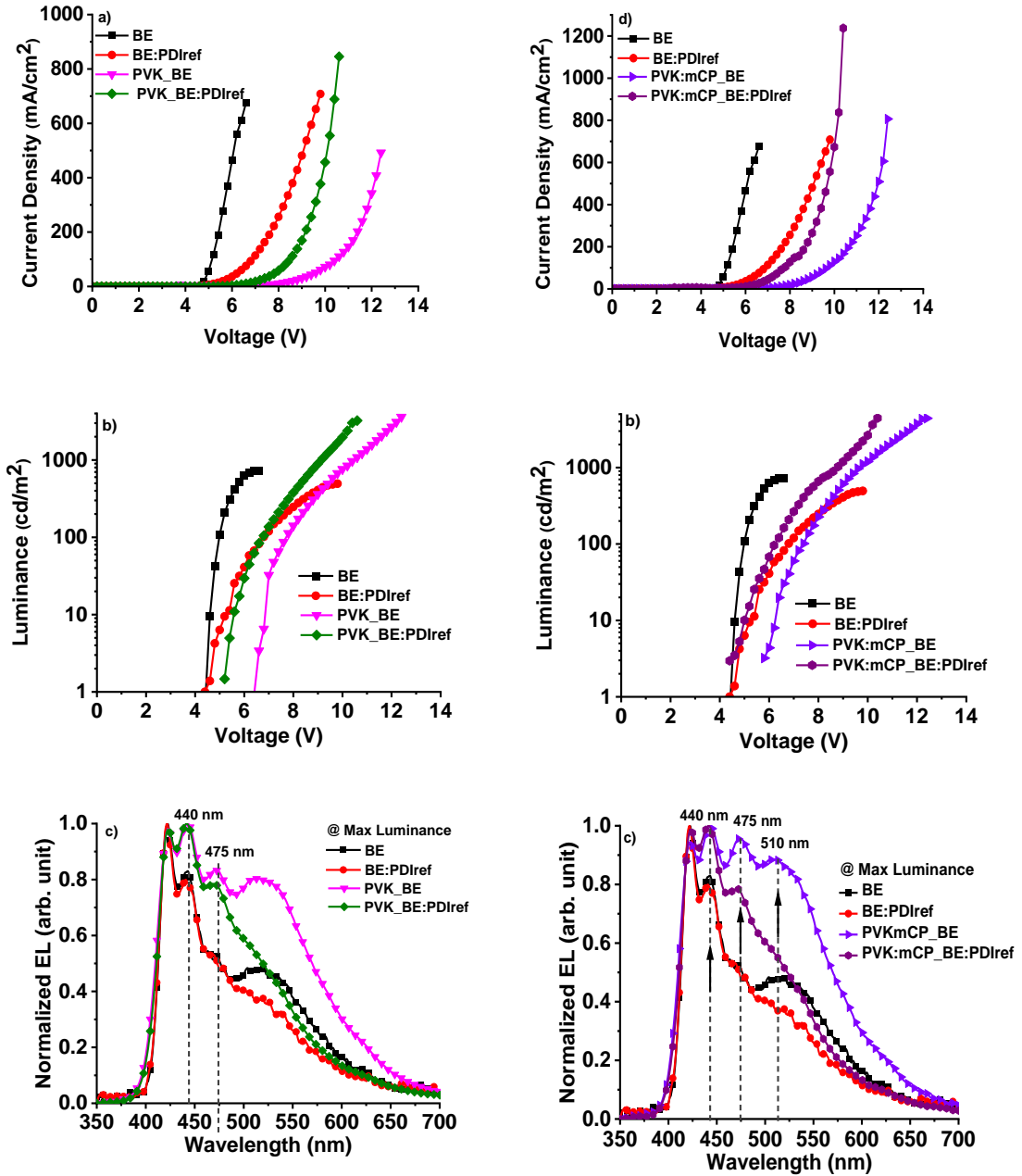


Figure 3.8. a) and d) current density, b and e) luminance vs applied voltage and c and f) normalized electroluminescence vs wavelength at maximum luminance characteristics of devices prepared by BE and PDIs doped BE emissive layer and PVK and PVK: mCP hole transport layers.

PVK (μh^+ : $2.5 \times 10^{-6} \text{ cm}^2\text{V}^{-1}\text{s}^{-1}$) (Junekyun Park et al. 2020), mCP (μh^+ : $1.2 \times 10^{-4} \text{ cm}^2\text{V}^{-1}\text{s}^{-1}$) (Z. Liu et al. 2020) and PVK:mCP (3:1) (μh^+ : $1 \times 10^{-3} \text{ cm}^2\text{V}^{-1}\text{s}^{-1}$) (measured by Volkan Bozkuş) by HTLs with different hole mobilities were used for the developed devices. The devices produced in the previous device study were determined as 3 reference devices, as shown in Figure 3.7. The remaining devices were devices with PVK

and PVK:mCP HTL layers. Comparing PDiref with PDI1 doping, the situation is similar for both HTLs. When PDiref and PDI1 doping is taken into account, it is seen that there is an approach to the deep blue in the CIE coordinates and a narrowing of the FWHM around 50 nm, on the other hand, the turn-on voltage has increased Figure 3.8c. As expected, there was a relative decrease in efficiency and luminance values as purification occurred in blue light production. The effect of PDI1, on the other hand, is not very different in terms of CIE coordinates with decreases in yields and luminance values (Figure 3.8, A.7 and A.8).

Table 3.3. Electroluminescence efficiencies were evaluated for BE and PDIs-doped BE layers as emissive layer and PVK and PVK:mCP layers as hole transport layer.

HTL	EML	Lum _{max} (cd/m ²)	Turn-on (V)	PE (lm/W)	CE (cd/A)	EQE (%)	CIE (x, y)	FWHM (nm)
-	BE	732	4.4	0.15	0.23	0.13	(0.22, 0.25)	46
	BE:PDiref	494	4.4	0.07	0.13	0.08	(0.20, 0.21)	51
PVK	BE	3610	6.8	0.57	1.36	0.60	(0.24, 0.30)	160
	BE:PDiref	3235	5.2	0.58	1.04	0.53	(0.20, 0.22)	109
PVK:mCP (3:1)	BE	4412	5.7	0.59	1.27	0.57	(0.23, 0.30)	160
	BE:PDiref	4440	4.2	0.36	0.65	0.40	(0.20, 0.22)	113

The HTLs were improved interface between PEDOT:PSS and EML and enabled to more hole transport to EML that resulted radiative combination. The charge balance was enhanced and the efficiencies and luminance were increased, as expected. To understand the effect of the addition of HTL in morphology and molecular structure AFM analysis and Raman measurements were studied.

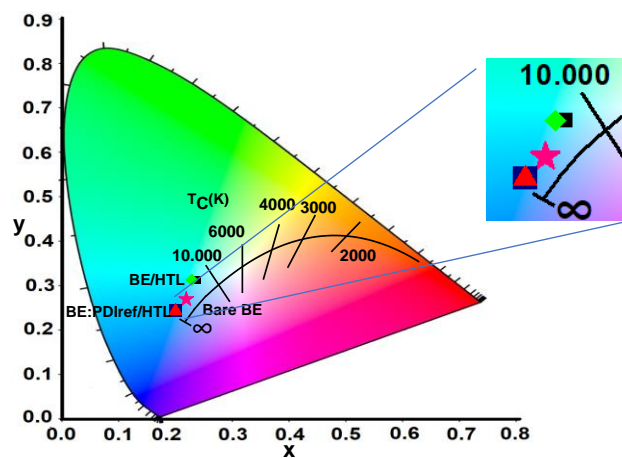


Figure 3.9. CIE coordinates of fabricated devices.

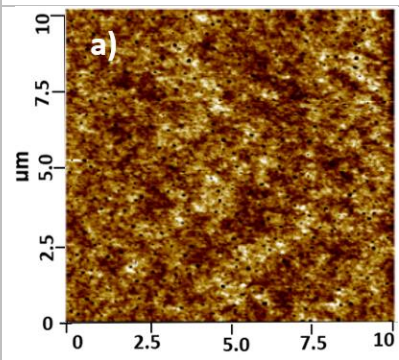
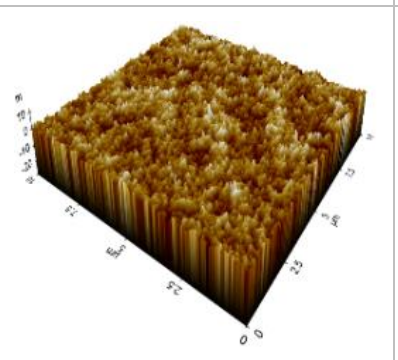
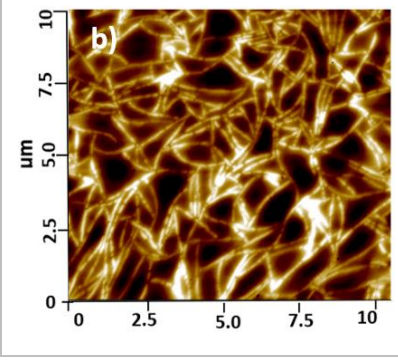
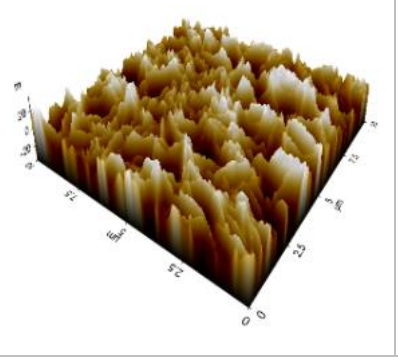
3.2.2. Morphological Analysis

Surface morphology is one of the most important factors affecting the charge flow within the device. It is well known that the morphology of organic semiconductors is influenced by the solvent, the annealing temperature and the interaction between the layers (Kulkarni and Jenekhe 2003). Appropriate coating parameters have been investigated to improve the charge flow of the surface.

The images representing the samples prepared by spin-coated on mica substrate/PEDOT:PSS, PVK and PVK:mCP under the EMLs according to the coating conditions of the original devices are summarized in Table 3.4. And the thickness of the organic thin films was summarized in A.5 and they were spin coated on glass substrate and measured with optical profilometer. They were coated in glass substrate. Film thickness values of PEDOT:PSS, BE, BE:PDIref, BE:PDI1, PVK and PVK:mCP; 69.8 ± 3.2 , 85.3 ± 3 , 86.5 ± 30 , 83.3 ± 3 , 59.1 ± 20 and 53.0 ± 20 , respectively.

Upon examining their surface topography, morphological variations were observed in the samples for both of HTL materials. On the surfaces of PVK, there is homogenous π - π stacking, resulting in lower roughness values of almost 1.5 nm. In previous study, there is a homogeneity in the morphology of BE, which occurs at 150°C, in Tol contrary to CB (Table 2.4). When PDI doped, the morphology of the material changes as shown in Table 3.2. Therefore, morphological changes have occurred in the perylene-doped thin films. But at last, the average roughness is maximum in PVK:mCP and BE:PDIref. In this device structure the luminance is maximum but efficiencies are not the best, as depicted.

Table 3.4. AFM images of PDIref doped PFO-POSS based OLEDs with HTLs.

HTL	2D	3D	Ra (nm)
PVK			1.479
PVK:mCP			8.935

This fibrous aggregation type of HTL added device structures it can not only be an improvement morphology changing, but also can be an improvement of aggregation type of EML. Instrumental analysis is needed to explain of the film topography. They were examined using Raman analysis in the A.9. The Raman spectra showed the identically trending with without HTL samples. In the high wavenumber region between $1650-1000\text{ cm}^{-1}$, the peaks shifted and intensity changing were almost the same. On the other hand, the intensity changing in low wave number region between $400-800\text{ cm}^{-1}$ were decreased from without HTL to PVK:mCP. That means, the movement of side chain was more reduced in PVK:mCP, while the main chain movement were stayed constant. This situation can be explained with more stable j-aggregation occurring, can be clearly seen in Table 3.4b. The presence of the HTL has enhanced the surface morphology of the emission layer.

CONCLUSION

The polymeric blue emitter ADS231BE is known for its solubility and cost-reducing potential. It faces challenges such as wide EL leading to color purity issues. The fabrication of a typical OLED using ADS231BE as the emitter material reveals that, regardless of the solvent used, efficiencies decrease gradually with annealing temperature. However, stability and color purity significantly improve with higher annealing temperatures. Examination of surface morphologies identifies optimal coating conditions, including a nitrogen atmosphere, toluene solvent, and a 150°C annealing temperature.

The introduction of small molecule orange-red-emitting PDI derivatives into ADS231BE at 0.1 wt.% concentration facilitates Förster-type energy transfer. Comprehensive analyses of electroluminescence, morphology, photoluminescence, and Raman aim to understand the aggregation type and conformational changes induced by PDI doping.

To enhance device characteristics, a hole transfer layer (HTL) comprising PVK and PVK:mCP is added. Similar morphological and Raman analyses are performed on the developed devices. The luminance value investigated from 494 cd to 4440cd per square meter and the external quantum efficiency enhanced from 0.08% to 0.40% when Δx coordinate is zero and Δy CIE coordinate 0.02.

LIST OF REFERENCES

- Abbel, Robert, Christophe Grenier, Maarten J Pouderoijen, Jan W Stouwdam, Philippe E L G Leclère, Rint P Sijbesma, E W Meijer, and Albertus P H J Schenning. 2018. “White-Light Emitting Hydrogen-Bonded Supramolecular Copolymers Based on π -Conjugated Oligomers.” <https://doi.org/https://doi.org/10.1021/ja807996y>.
- Abbel, Robert, Christophe Grenier, Maarten J. Pouderoijen, Jan W. Stouwdam, Philippe E.L.G. Leclère, Rint P. Sijbesma, E. W. Meijer, and Albertus P.H.J. Schenning. 2009. “White-Light Emitting Hydrogen-Bonded Supramolecular Copolymers Based on π -Conjugated Oligomers.” *Journal of the American Chemical Society* 131 (2): 833–43. <https://doi.org/10.1021/ja807996y>.
- Admassie, Shimelis, Olle Inganäs, Wendimagegn Mammo, Erik Perzon, and Mats R. Andersson. 2006. “Electrochemical and Optical Studies of the Band Gaps of Alternating Polyfluorene Copolymers.” *Synthetic Metals* 156 (7–8): 614–23. <https://doi.org/10.1016/j.synthmet.2006.02.013>.
- “ADS231BE.” n.d. Accessed December 4, 2023. <https://adsdyes.com/products/oled-pled/homopolymers-and-copolymers/ads231be/>.
- Aksoy, Erkan. 2020. “Organik Fotonik Sistemlerde Kullanılabilecek Perilen Diimit Türevlerinin Sentezi ve Fotofiziksel Karakterizasyonu.” Doktora Tezi, Ege Üniversitesi, İzmir.
- Alsop, Thomas. n.d. “Semiconductor Industry Revenue Worldwide from 2012 to 2024.”
- Bai, Lubing, Bin Liu, Yamin Han, Mengna Yu, Jiong Wang, Xinwen Zhang, Changjin Ou, et al. 2017. “Steric-Hindrance-Functionalized Polydiarylflorenes: Conformational Behavior, Stabilized Blue Electroluminescence, and Efficient Amplified Spontaneous Emission.” *ACS Applied Materials and Interfaces* 9 (43): 37856–63. <https://doi.org/10.1021/acsami.7b08980>.
- Ban, Xinxin, Kaiyong Sun, Yueming Sun, Bin Huang, and Wei Jiang. 2016. “Enhanced Electron Affinity and Exciton Confinement in Exciplex-Type Host: Power Efficient Solution-Processed Blue Phosphorescent OLEDs with Low Turn-on Voltage.” *ACS Applied Materials and Interfaces* 8 (3): 2010–16. <https://doi.org/10.1021/acsami.5b10335>.
- Beigmohamadi, M., P. Niyamakom, A. Farahzadi, C. Effertz, S. Kremers, D. Brueggemann, and M. Wuttig. 2008. “Structure and Morphology of Perylene Films Grown on Different Substrates.” *Journal of Applied Physics* 104 (1). <https://doi.org/10.1063/1.2951900>.
- Bharathan, Jayesh, and Yang Yang. 1998. “Polymer Electroluminescent Devices Processed by Inkjet Printing: I. Polymer Light-Emitting Logo.” *Applied Physics Letters* 72 (21): 2660–62. <https://doi.org/10.1063/1.121090>.

- Birks, J.B., J.H. Appleyard, and Rosalind Pope. 1936. "The Photo-Dimers Of Anthracene, Tetracene And Pentacene." *Photochemistry and Photobiology* V.2 (July): 493–95. <https://doi.org/10.1039/C5CC09481J>.
- Bozkus, Volkan, Erkan Aksoy, and Canan Varlikli. 2021. "Perylene Based Solution Processed Single Layer WOLED with Adjustable CCT and CRI." *Electronics (Switzerland)* 10 (6): 1–12. <https://doi.org/10.3390/electronics10060725>.
- Brown, T. M., J. S. Kim, R. H. Friend, F. Cacialli, R. Daik, and W. J. Feast. 1999. "Built-in Field Electroabsorption Spectroscopy of Polymer Light-Emitting Diodes Incorporating a Doped Poly(3,4-Ethylene Dioxythiophene) Hole Injection Layer." *Applied Physics Letters* 75 (12): 1679–81. <https://doi.org/10.1063/1.124789>.
- Campbell, A. J., W. Blau, P. A. Lane, L. C. Palilis, A. J. Cadby, D. D.C. Bradley, C. Giebeler, D. G. Lidzey, and D. F. O'Brien. 2001. "Origin of Electrophosphorescence from a Doped Polymer Light Emitting Diode." *Physical Review B - Condensed Matter and Materials Physics* 63 (23). <https://doi.org/10.1103/PhysRevB.63.235206>.
- Chang, Huan, Zhiming Chen, Xiye Yang, Qingwu Yin, Jie Zhang, Lei Ying, Xiao Fang Jiang, Baomin Xu, Fei Huang, and Yong Cao. 2017. "Novel Perylene Diimide Based Polymeric Electron-Acceptors Containing Ethynyl as the π -Bridge for All-Polymer Solar Cells." *Organic Electronics* 45 (June): 227–33. <https://doi.org/10.1016/j.orgel.2017.03.022>.
- Chen, Liaohai, Lucian A. Lucia, E. R. Gaillard, David G. Whitten, H. Icil, and S. Icli. 1998. "Photooxidation of a Conjugated Diene by an Exciplex Mechanism: Amplification via Radical Chain Reactions in the Perylene Diimide-Photosensitized Oxidation of α -Terpinene." *Journal of Physical Chemistry A* 102 (45): 9095–98. <https://doi.org/10.1021/jp983346t>.
- Cormier, Russell A, and Brian A Gregg. 1997. "Self-Organization in Thin Films of Liquid Crystalline Perylene Diimides." *Journal of Physics Chemistry* 101 (51): 11004–6. <https://doi.org/10.1021/jp9732064>.
- Dayneko, Sergey V., Edward Cieplechowicz, Sachin Suresh Bhojgude, Jeffrey F. Van Humbeck, Majid Pahlevani, and Gregory C. Welch. 2021. "Improved Performance of Solution Processed OLEDs Using: N -Annulated Perylene Diimide Emitters with Bulky Side-Chains." *Materials Advances* 2 (3): 933–36. <https://doi.org/10.1039/d0ma00827c>.
- Dayneko, Sergey V., Mohammad Rahmati, Majid Pahlevani, and Gregory C. Welch. 2020. "Solution Processed Red Organic Light-Emitting-Diodes Using an: N-Annulated Perylene Diimide Fluorophore." *Journal of Materials Chemistry C* 8 (7): 2314–19. <https://doi.org/10.1039/c9tc05584c>.
- Demir, Nuriye. 2014. "Sarı ve Mavi Işıma Yapan Konjuge Polimer-CuInS₂ Kuantum Parçacığı Hibritlerinde Foto-Fiziksel Davranışların Tespiti ve OLED Uygulamaları."

- Deng, Yonghong, Wen Yuan, Zhe Jia, and Gao Liu. 2014. "H- and J-Aggregation of Fluorene-Based Chromophores." *Journal of Physical Chemistry B* 118 (49): 14536–45. <https://doi.org/10.1021/jp510520m>.
- Diker, Halide, Fatih Yesil, and Canan Varlikli. 2019. "Contribution of O₂ Plasma Treatment and Amine Modified GOs on Film Properties of Conductive PEDOT:PSS: Application in Indium Tin Oxide Free Solution Processed Blue OLED." *Current Applied Physics* 19 (8): 910–16. <https://doi.org/10.1016/j.cap.2019.04.018>.
- Drexler, K. Eric. 2004. "Nanotechnology: From Feynman to Funding." *Bulletin of Science, Technology and Society* 24 (1): 21–27. <https://doi.org/10.1177/0270467604263113>.
- Duarte, Luís Gustavo T.A., José Carlos Germino, Rodrigo A. Mendes, Jônatas F. Berbigier, Marcelo M. Faleiros, Fabiano S. Rodembusch, and Teresa D.Z. Atvars. 2019a. "The Role of a Simple and Effective Salicylidene Derivative. Spectral Broadening and Performance Improvement of PFO-Based All-Solution Processed OLEDs." *Dyes and Pigments* 171 (December). <https://doi.org/10.1016/j.dyepig.2019.107671>.
- Fan, Suqin, Mingliang Sun, Jian Wang, Wei Yang, and Yong Cao. 2007. "Efficient White-Light-Emitting Diodes Based on Polyfluorene Doped with Fluorescent Chromophores." *Applied Physics Letters* 91 (21). <https://doi.org/10.1063/1.2812569>.
- Feng, Quanyou, Songlin Xie, Kesheng Tan, Xiaojun Zheng, Zhitao Yu, Lianjie Li, Bin Liu, et al. 2019a. "Conjugated Nanopolymer Based on a Nanogrid: Approach toward Stable Polyfluorene-Type Fluorescent Emitter for Blue Polymer Light-Emitting Diodes." *ACS Applied Polymer Materials* 1 (9): 2441–49. <https://doi.org/10.1021/acsapm.9b00559>.
- Gong, Su Cheol, and Ho Jung Chang. 2009. "Low Temperature Annealing Effect of PFO-Poss Emission Layer on the Properties of Polymer Light Emitting Diodes." *Korean Journal of Materials Research* 19 (6): 313–18. <https://doi.org/10.3740/MRSK.2009.19.6.313>.
- Görl, Daniel, Xin Zhang, Vladimir Stepanenko, and Frank Würthner. 2015. "Supramolecular Block Copolymers by Kinetically Controlled Co-Self-Assembly of Planar and Core-Twisted Perylene Bisimides." *Nature Communications* 6 (May). <https://doi.org/10.1038/ncomms8009>.
- Grice, A. W., D. D.C. Bradley, M. T. Bernius, M. Inbasekaran, W. W. Wu, and E. P. Woo. 1998. "High Brightness and Efficiency Blue Light-Emitting Polymer Diodes." *Applied Physics Letters* 73 (5): 629–31. <https://doi.org/10.1063/1.121878>.
- Gross, M, D. C. Müller, H. G. Nothofer, U. Scherf, D. Neher, C. Brauchle, and K. Meerholz. 2000. "Improving the Performance of Doped P-Conjugated Polymers for Use in Organic Light-Emitting Diodes." *Nature* VOL 405 (April): 661–65. <https://doi.org/https://doi.org/10.1038/35015037>.

- Hong, Gloria, Xuemin Gan, Céline Leonhardt, Zhen Zhang, Jasmin Seibert, Jasmin M. Busch, and Stefan Bräse. 2021. “A Brief History of OLEDs—Emitter Development and Industry Milestones.” *Advanced Materials* 33 (9). <https://doi.org/10.1002/adma.202005630>.
- Hu, Liwen, Junfei Liang, Wenkai Zhong, Ting Guo, Zhiming Zhong, Feng Peng, Baobing Fan, Lei Ying, and Yong Cao. 2019a. “Improving the Electroluminescence Performance of Blue Light-Emitting Poly(Fluorene-Co-Dibenzothiophene- S, S -Dioxide) by Tuning the Intra-Molecular Charge Transfer Effects and Temperature-Induced Orientation of the Emissive Layer Structure.” *Journal of Materials Chemistry C* 7 (19): 5630–38. <https://doi.org/10.1039/c9tc00842j>.
- Hu, Liwen, Zhonglian Wu, Xiaojun Wang, Yawei Ma, Ting Guo, Lei Ying, Junbiao Peng, and Yong Cao. 2019. “Deep-Blue Light-Emitting Polyfluorenes with Asymmetrical Naphthylthio-Fluorene as Chromophores.” *Journal of Polymer Science, Part A: Polymer Chemistry* 57 (2): 171–82. <https://doi.org/10.1002/pola.29283>.
- Hu, Shu, Yang Liao, Yang Zhang, Xiaoliang Yan, Zhenlu Zhao, Weiqiang Chen, Xin Zhang, et al. 2020. “Effect of Thermal Annealing on Conformation of Meh-Ppv Chains in Polymer Matrix: Coexistence of H-and J-Aggregates.” *Polymers* 12 (8). <https://doi.org/10.3390/polym12081771>.
- Huang, Long, Xinan Huang, Guannan Sun, Cheng Gu, Dan Lu, and Yuguang Ma. 2012. “Study of β Phase and Chains Aggregation Degrees in Poly(9,9-Dioctylfluorene) (PFO) Solution.” *Journal of Physical Chemistry C* 116 (14): 7993–99. <https://doi.org/10.1021/jp301102t>.
- Huang, Zhiqi, Zhaoxi Fu, Jin Xu, Feng Peng, Ting Guo, and Lei Ying. 2020. “Efficient Deep-Blue Light-Emitting Polyfluorenes Based on 9,9-Dimethyl-9H-Thioxanthene 10,10-Dioxide Isomers.” *Journal of Polymer Science* 58 (10): 1380–92. <https://doi.org/10.1002/pol.20200114>.
- Icil, Huriye. 1998. “Energy Transfer Studies with Perylene Bis-Diimide Derivatives.” *Spectroscopy Letters* 31 (4): 747–55. <https://doi.org/10.1080/00387019808007396>.
- Jadoun, Sapana, and Ufana Riaz. 2020. “Conjugated Polymer Light-Emitting Diodes.” *Polymers for Light-Emitting Devices and Displays*, 77–98. <https://doi.org/https://doi.org/10.1002/9781119654643.ch4>.
- Jokinen, K., A. Bykov, R. Sliz, K. Remes, T. Fabritius, and R. Myllylä. 2015. “Luminescence and Spectrum Variations Caused by Thermal Annealing in Undoped and Doped Polyfluorene OLEDs.” *Solid-State Electronics* 103: 184–89. <https://doi.org/10.1016/j.sse.2014.07.015>.
- Ju, So Eun, Chang Gi Yoon, and Jiwan Kim. 2020. “Hybrid Electroluminescence Devices with Solution-Processed Mixed Emitting Layers of Red Quantum Dots and Blue Small Molecules.” *Coatings* 10 (7). <https://doi.org/10.3390/coatings10070645>.

- Kasha, M, H R Rawls, and M Ashraf El-Bayoumi. 2009. "The Exciton Model In Molecular Spectroscopy." *Pure and Applied Chemistry* 11 (3–4): 371–92. <https://doi.org/https://doi.org/10.1351/pac196511030371>.
- Katz, H E, Z Bao, H Sirringhaus, P J Brown, R H Friend, M M Nielsen, K Bechgaard, et al. 2000. "The Effect of Keto Defect Sites on the Emission of Polyfluorene-Type Materials." *J. Polym. Sci., Part B: Polym. Phys* 104 (5): 149. [https://doi.org/https://doi.org/10.1002/1521-4095\(20020304\)14:5<374::AID-ADMA374>3.0.CO;2-U](https://doi.org/https://doi.org/10.1002/1521-4095(20020304)14:5<374::AID-ADMA374>3.0.CO;2-U).
- Kulkarni, Abhishek P., and Samson A. Jenekhe. 2003. "Blue Light-Emitting Diodes with Good Spectral Stability Based on Blends of Poly(9,9-Dioctylfluorene): Interplay between Morphology, Photophysics, and Device Performance." *Macromolecules* 36 (14): 5285–96. <https://doi.org/10.1021/ma0344700>.
- Li, Lu, Tian Qing Hu, Cheng Rong Yin, Ling Hai Xie, Yang Yang, Chao Wang, Jin Yi Lin, Ming Dong Yi, Shang Hui Ye, and Wei Huang. 2015. "A Photo-Stable and Electrochemically Stable Poly(Dumbbell-Shaped Molecules) for Blue Electrophosphorescent Host Materials." *Polymer Chemistry* 6 (6): 983–88. <https://doi.org/10.1039/c4py01016g>.
- Li, Tao, Bin Liu, Hao Zhang, Jiakuan Ren, Zeming Bai, Xiaona Li, Tengning Ma, and Dan Lu. 2016. "Effect of Conjugated Polymer Poly (9,9-Dioctylfluorene) (PFO) Molecular Weight Change on the Single Chains, Aggregation and β Phase." *Polymer* 103 (October): 299–306. <https://doi.org/10.1016/j.polymer.2016.09.072>.
- Li, Yi, Xin Ling Zhang, and Di Liu. 2021. "Recent Developments of Perylene Diimide (PDI) Supramolecular Photocatalysts: A Review." *Journal of Photochemistry and Photobiology C: Photochemistry Reviews*. Elsevier B.V. <https://doi.org/10.1016/j.jphotochemrev.2021.100436>.
- Lighting Equipment Sales. n.d. "Structure of Conventional OLED Device." Accessed January 4, 2024. <https://lightingequipmentsales.com/oled.html>.
- Lin, Ying, Teng Ling Ye, Yu Chen, Dong Ge Ma, Zhi Kuan Chen, Yan Feng Dai, and Yong Xi Li. 2010. "Blue-Light-Emitting Polyfluorene Functionalized with Triphenylamine and Cyanophenylfluorene Bipolar Side Chains." *Journal of Polymer Science, Part A: Polymer Chemistry* 48 (24): 5930–37. <https://doi.org/10.1002/pola.24406>.
- Lin, Yuze, and Xiaowei Zhan. 2015. "Designing Efficient Non-Fullerene Acceptors by Tailoring Extended Fused-Rings with Electron-Deficient Groups." *Advanced Energy Materials* 5 (20). <https://doi.org/10.1002/aenm.201501063>.
- Liu, Bin, Zeming Bai, Tao Li, Yang Liu, Xiaona Li, Hao Zhang, and Dan Lu. 2019. "Discovery and Structure Characteristics of the Intermediate-State Conformation of Poly(9,9-Dioctylfluorene) (PFO) in the Dynamic Process of Conformation Transformation and Its Effects on Carrier Mobility." *RSC Advances* 10 (1): 492–500. <https://doi.org/10.1039/c9ra07115f>.

- Liu, Bin, Hao Zhang, Jiakuan Ren, Tengning Ma, Mengna Yu, Linghai Xie, and Dan Lu. 2019. "Effect of Solvent Aromaticity on Poly(9,9-Dioctylfluorene) (PFO) Chain Solution Behavior and Film Condensed State Structure." *Polymer* 185 (December). <https://doi.org/10.1016/j.polymer.2019.121986>.
- Liu, Jian, Li Qiu, Riccardo Alessandri, Xinkai Qiu, Giuseppe Portale, Jing Jin Dong, Wytse Talsma, et al. 2018. "Enhancing Molecular N-Type Doping of Donor–Acceptor Copolymers by Tailoring Side Chains." *Advanced Materials* 30 (7). <https://doi.org/10.1002/adma.201704630>.
- Liu, Ya Di, Qiang Zhang, Xin Hong Yu, Jian Gang Liu, and Yan Chun Han. 2019. "Increasing the Content of β Phase of Poly(9,9-Dioctylfluorene) by Synergistically Controlling Solution Aggregation and Extending Film-Forming Time." *Chinese Journal of Polymer Science (English Edition)* 37 (7): 664–73. <https://doi.org/10.1007/s10118-019-2259-3>.
- Liu, Zijian, Wei Ye Zheng, Peng Wei, Zheng Xu, Dandan Song, Bo Qiao, and Suling Zhao. 2020. "The Improved Performance and Mechanism of Solution-Processed Blue PhOLEDs Based on Double Electron Transport Layers." *RSC Advances* 10 (22): 13215–22. <https://doi.org/10.1039/d0ra00515k>.
- Lova, Paola, Vincenzo Grande, Giovanni Manfredi, Maddalena Patrini, Stefanie Herbst, Frank Würthner, and Davide Comoretto. 2017a. "All-Polymer Photonic Microcavities Doped with Perylene Bisimide J-Aggregates." *Advanced Optical Materials* 5 (21). <https://doi.org/10.1002/adom.201700523>.
- Lu, Yang, Jie Yu Wang, and Jian Pei. 2021. "Achieving Efficient N-Doping of Conjugated Polymers by Molecular Dopants." *Accounts of Chemical Research* 54 (13): 2871–83. <https://doi.org/10.1021/acs.accounts.1c00223>.
- Matussek, Marek, Michał Filapek, Paweł Gancarz, Stanisław Krompiec, Jan Grzegorz Małecki, Sonia Kotowicz, Mariola Siwy, et al. 2018. "Synthesis and Photophysical Properties of New Perylene Bisimide Derivatives for Application as Emitting Materials in OLEDs." *Dyes and Pigments* 159 (December): 590–99. <https://doi.org/10.1016/j.dyepig.2018.07.006>.
- Moliton, André, and Roger C. Hiorns. 2012. "The Origin and Development of (Plastic) Organic Electronics." *Polymer International*. <https://doi.org/10.1002/pi.4173>.
- Morais, Andreia de, Wesley de Souza Rodrigues, Douglas José Coutinho, Ana Flávia Nogueira, and Jilian Nei de Freitas. 2023. "Investigation of Nitrogen-Doped Carbon Dot/ZnO Nanocomposites and Their Application as Interlayer in Solution-Processed Organic Light Emitting Diodes." *Materials Science and Engineering: B* 297 (November). <https://doi.org/10.1016/j.mseb.2023.116749>.
- MSI. 2019. "The Color Space on CIE 1931 Chromaticity Diagram." January 3, 2019. <https://www.msi.com/blog/why-dci-p3-is-the-new-standard-of-color-gamut>.
- Ohmori, Y., M. Uchida, Muro K., and Yoshino K. 1991. "Blue Electroluminescent Diodes Utilizing Poly(Alkylfluorene)." *Japanese Journal of Applied Physics* VOL. 30: L1941–43. <https://doi.org/10.1143/JJAP.30.L1941>.

- Oide, Mariane Y T, Herick G Takimoto, Emerson R Santos, Ana L Silva, Nakédia M F Carvalho, Roberto K Onmori, and Shu H Wang. 2023. "Impact of the Green Phosphorescent Ir(Ppy) 3 on the Optical and Electrical Properties of Blue-Emitting Polymers with Different Bandgaps," October. <https://doi.org/https://dx.doi.org/10.2139/ssrn.4615804>.
- Ostroverkhova, Oksana. 2016. "Organic Optoelectronic Materials: Mechanisms and Applications." *Chemical Reviews* 116 (22): 13279–412. <https://doi.org/10.1021/acs.chemrev.6b00127>.
- Pal, Arindam, Murali Gedda, and Dipak K. Goswami. 2022. "PTCDI-Ph Molecular Layer Stack-Based Highly Crystalline Microneedles As Single-Component Efficient Photodetector." *ACS Applied Electronic Materials* 4 (3): 946–54. <https://doi.org/10.1021/acsaelm.1c01068>.
- Pan, Jiangyong, Jing Chen, Qianqian Huang, Lixi Wang, and Wei Lei. 2017. "A Highly Efficient Quantum Dot Light Emitting Diode: Via Improving the Carrier Balance by Modulating the Hole Transport." *RSC Advances* 7 (69): 43366–72. <https://doi.org/10.1039/c7ra08302e>.
- Park, Jihun, Sanghyun Heo, Kibog Park, Myoung Hoon Song, Ju Young Kim, Gyouhyung Kyung, Rodney Scott Ruoff, Jang Ung Park, and Franklin Bien. 2017. "Research on Flexible Display at Ulsan National Institute of Science and Technology." *Npj Flexible Electronics* 1 (1). <https://doi.org/10.1038/s41528-017-0006-9>.
- Park, Junekyun, Eunkyun Shin, Jongwoo Park, and Yonghan Roh. 2020. "Improvement of Quantum Dot Light Emitting Device Characteristics by CdSe/ZnS Blended with HMDS (Hexamethyldisilazane)." *Applied Sciences (Switzerland)* 10 (17). <https://doi.org/10.3390/app10176081>.
- Peng, Feng, Wenkai Zhong, Zhiming Zhong, Ting Guo, and Lei Ying. 2020. "Improving the Electroluminescent Performance of Blue Light-Emitting Polymers by Side-Chain Modification." *ACS Applied Materials and Interfaces* 12 (7): 8495–8502. <https://doi.org/10.1021/acsami.9b21652>.
- Sasabe, Hisahiro, and Junji Kido. 2013. "Development of High Performance OLEDs for General Lighting." *Journal of Materials Chemistry C* 1 (9): 1699–1707. <https://doi.org/10.1039/c2tc00584k>.
- Schols, Sarah. 2011. *Device Architecture and Materials for Organic Light-Emitting Devices*. Device Architecture and Materials for Organic Light-Emitting Devices. Springer Netherlands. <https://doi.org/10.1007/978-94-007-1608-7>.
- Sevim, Secil, Gorkem Memisoglu, Canan Varlikli, Leyla Eral Doğan, Didem Tascioglu, and Serdar Ozelik. 2014. "An Ultraviolet Photodetector with an Active Layer Composed of Solution Processed Polyfluorene:Zn 0.71 Cd 0.29 S Hybrid

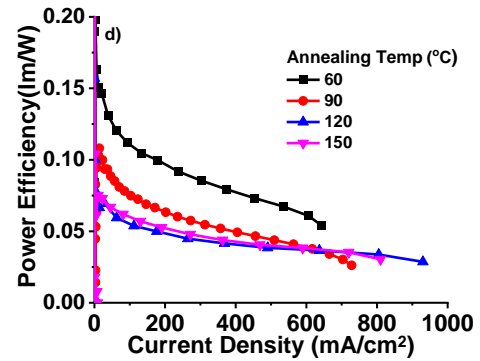
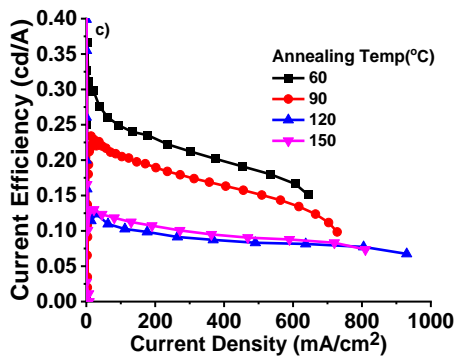
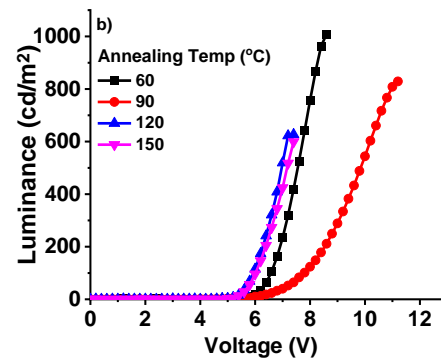
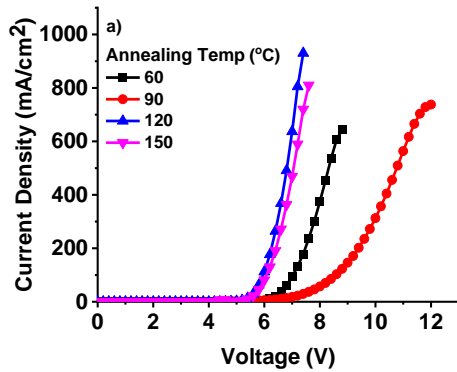
- Nanomaterials.” *Applied Surface Science* 305 (June): 227–34. <https://doi.org/10.1016/j.apsusc.2014.03.042>.
- Shannon, C E. 1948. “A Mathematical Theory of Communication.” *The Bell System Technical Journal*.
- Shaw, J.M, and P.F. Seidler. 2001. “Organic Electronics: Introduction.” *IBM Journal of Research and Development* VOL. 45: 3–9. <https://doi.org/10.1147/rd.451.0003>.
- Shu, Ching Fong, Rajasekhar Dodda, Fang Iy Wu, Michelle S. Liu, and Alex K.Y. Jen. 2003. “Highly Efficient Blue-Light-Emitting Diodes from Polyfluorene Containing Bipolar Pendant Groups.” *Macromolecules* 36 (18): 6698–6703. <https://doi.org/10.1021/ma030123e>.
- Spano, Frank C., and Carlos Silva. 2014. “H- and J-Aggregate Behavior in Polymeric Semiconductors.” *Annual Review of Physical Chemistry* 65: 477–500. <https://doi.org/10.1146/annurev-physchem-040513-103639>.
- Tang, C. W., and S. A. Vanslyke. 1987. “Organic Electroluminescent Diodes.” *Applied Physics Letters* 51 (12): 913–15. <https://doi.org/10.1063/1.98799>.
- Tasch, S., E. J.W. List, O. Ekström, W. Graupner, G. Leising, P. Schlichting, U. Rohr, Y. Geerts, U. Schert, and K. Müllen. 1997. “Efficient White Light-Emitting Diodes Realized with New Processable Blends of Conjugated Polymers.” *Applied Physics Letters* 71 (20): 2883–85. <https://doi.org/10.1063/1.120205>.
- Tischler, Jonathan R., M. Scott Bradley, Vladimir Bulović, Jung Hoon Song, and Arto Nurmikko. 2005. “Strong Coupling in a Microcavity LED.” *Physical Review Letters* 95 (3). <https://doi.org/10.1103/PhysRevLett.95.036401>.
- Uoyama, Hiroki, Kenichi Goushi, Katsuyuki Shizu, Hiroko Nomura, and Chihaya Adachi. 2012. “Highly Efficient Organic Light-Emitting Diodes from Delayed Fluorescence.” *Nature* 492 (7428): 234–38. <https://doi.org/10.1038/nature11687>.
- Vavilov, V.S. 1994. “Physics and Applications of Wide Bandgap Semiconductors.” *Physics*, 269–77. <http://iopscience.iop.org/1063-7869/37/3/R03>.
- Waddon, Alan J., and E. Bryan Coughlin. 2003. “Crystal Structure of Polyhedral Oligomeric Silsequioxane (POSS) Nano-Materials: A Study by X-Ray Diffraction and Electron Microscopy.” *Chemistry of Materials* 15 (24): 4555–61. <https://doi.org/10.1021/cm034308b>.
- Wan, Li, Xingyuan Shi, Jessica Wade, Alasdair J. Campbell, and Matthew J. Fuchter. 2021. “Strongly Circularly Polarized Crystalline and β -Phase Emission from Poly(9,9-Dioctylfluorene)-Based Deep-Blue Light-Emitting Diodes.” *Advanced Optical Materials* 9 (19). <https://doi.org/10.1002/adom.202100066>.
- Weinfurtner, Karl Heinz, Hisayoshi Fujikawa, Shizuo Tokito, and Yasunori Taga. 2000. “Highly Efficient Pure Blue Electroluminescence from Polyfluorene: Influence of

- the Molecular Weight Distribution on the Aggregation Tendency.” *Applied Physics Letters* 76 (18): 2502–4. <https://doi.org/10.1063/1.126389>.
- Xiao, Steven, My Nguyen, Xiong Gong, Yong Cao, Hongbin Wu, Daniel Moses, and Alan J Heeger. 2003. “Stabilization of Semiconducting Polymers with Silsesquioxane**.” *Advanced Functional Materials* 13: 25–29.
- Xu, Jin, Feng Peng, Yong Yang, Liwen Hu, Ruifeng He, Wei Yang, and Yong Cao. 2017. “Highly Efficient Inverted Blue Light-Emitting Diodes by Thermal Annealing and Interfacial Modification.” *Organic Electronics* 49 (October): 1–8. <https://doi.org/10.1016/j.orgel.2017.05.039>.
- Xu, Yunhua, Junbiao Peng, Jiaying Jiang, Wei Xu, Wei Yang, and Yong Cao. 2005. “Efficient White-Light-Emitting Diodes Based on Polymer Codoped with Two Phosphorescent Dyes.” *Applied Physics Letters* 87 (19): 1–3. <https://doi.org/10.1063/1.2119407>.
- Yamagata, Hajime, and Frank C. Spano. 2014. “Strong Photophysical Similarities between Conjugated Polymers and J-Aggregates.” *Journal of Physical Chemistry Letters*. <https://doi.org/10.1021/jz402450m>.
- Yang, Liping, Pengyuan Wang, Jiao Yin, Chuanyi Wang, Guohui Dong, Yuanhao Wang, and Wingkei Ho. 2019. “Engineering of Reduced Graphene Oxide on Nanosheet–g-C₃N₄/Perylene Imide Heterojunction for Enhanced Photocatalytic Redox Performance.” *Applied Catalysis B: Environmental* 250 (August): 42–51. <https://doi.org/10.1016/j.apcatb.2019.02.076>.
- Yang, Wei, Qiong Hou, Chuanzhen Liu, Yuhua Niu, Jian Huang, Renqiang Yang, and Yong Cao. 2003. “Improvement of Color Purity in Blue-Emitting Polyfluorene by Copolymerization with Dibenzothiophene.” *Journal of Materials Chemistry* 13 (6): 1351–55. <https://doi.org/10.1039/b300202k>.
- Yeşil, Fatih. 2017. “İletken Geçirgen Oksit İçermeyen Mavi Organik Işık Yayan Diyotlarda Grafen Oksitin Etkilerinin Araştırılması.”
- Yu, Wang Lin, Yong Cao, Jian Pei, Wei Huang, and Alan J. Heeger. 1999. “Blue Polymer Light-Emitting Diodes from Poly(9,9-Dihexylfluorene-Alt-Co-2, 5-Didecyloxy-Para-Phenylene).” *Applied Physics Letters* 75 (21): 3270–72. <https://doi.org/10.1063/1.125321>.
- Zhang, Bolong, Hamid Soleimanejad, David J. Jones, Jonathan M. White, Kenneth P. Ghiggino, Trevor A. Smith, and Wallace W.H. Wong. 2017. “Highly Fluorescent Molecularly Insulated Perylene Diimides: Effect of Concentration on Photophysical Properties.” *Chemistry of Materials* 29 (19): 8395–8403. <https://doi.org/10.1021/acs.chemmater.7b02968>.
- Zhang, He Shan, Xue Mei Dong, Zi Cheng Zhang, Ze Pu Zhang, Chao Yi Ban, Zhe Zhou, Cheng Song, et al. 2022. “Co-Assembled Perylene/Graphene Oxide Photosensitive Heterobilayer for Efficient Neuromorphics.” *Nature Communications* 13 (1). <https://doi.org/10.1038/s41467-022-32725-y>

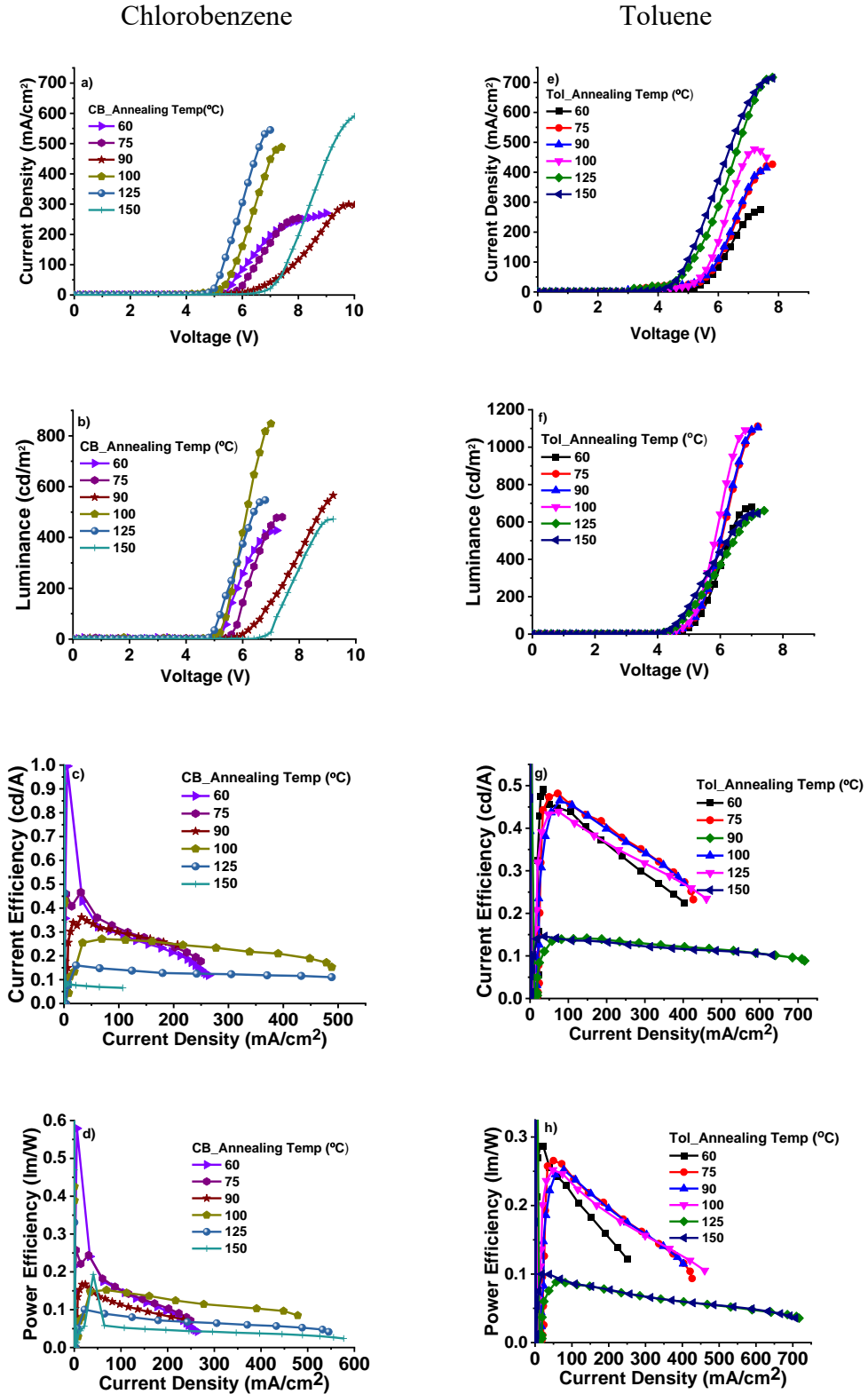
Zong, Luyi, Yanbin Gong, Yun Yu, Yujun Xie, Guohua Xie, Qian Peng, Qianqian Li, and Zhen Li. 2018. “New Perylene Diimide Derivatives: Stable Red Emission, Adjustable Property from ACQ to AIE, and Good Device Performance with an EQE Value of 4.93%.” *Science Bulletin* 63 (2): 108–16. <https://doi.org/10.1016/j.scib.2017.10.021>.

APPENDIX A

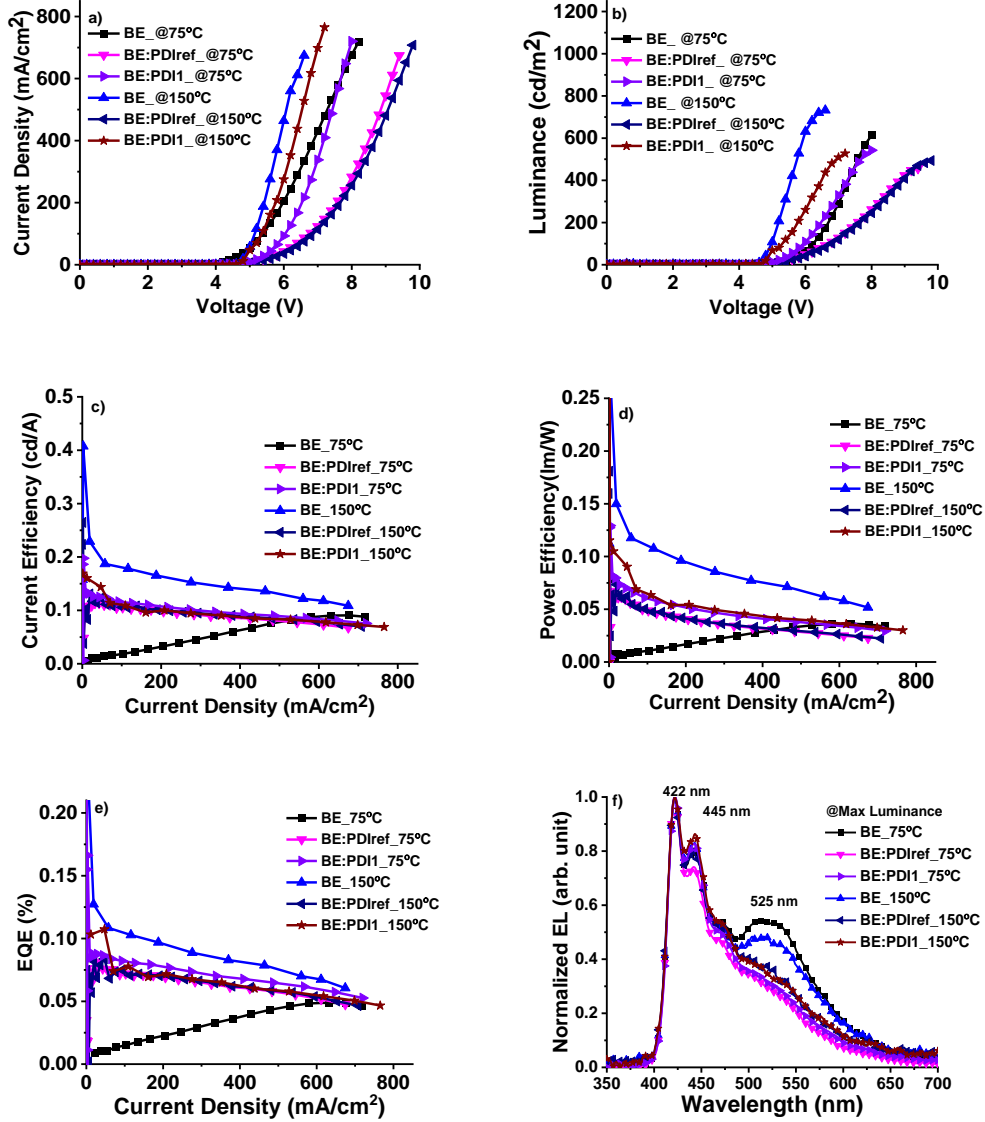
A.1. a) current density, b) luminescence vs voltage and, c) current efficiency and d) power efficiency vs current density characteristics of devices annealed at different temperatures and prepared by coating with chlorobenzene solvent in air atmosphere, respectively.



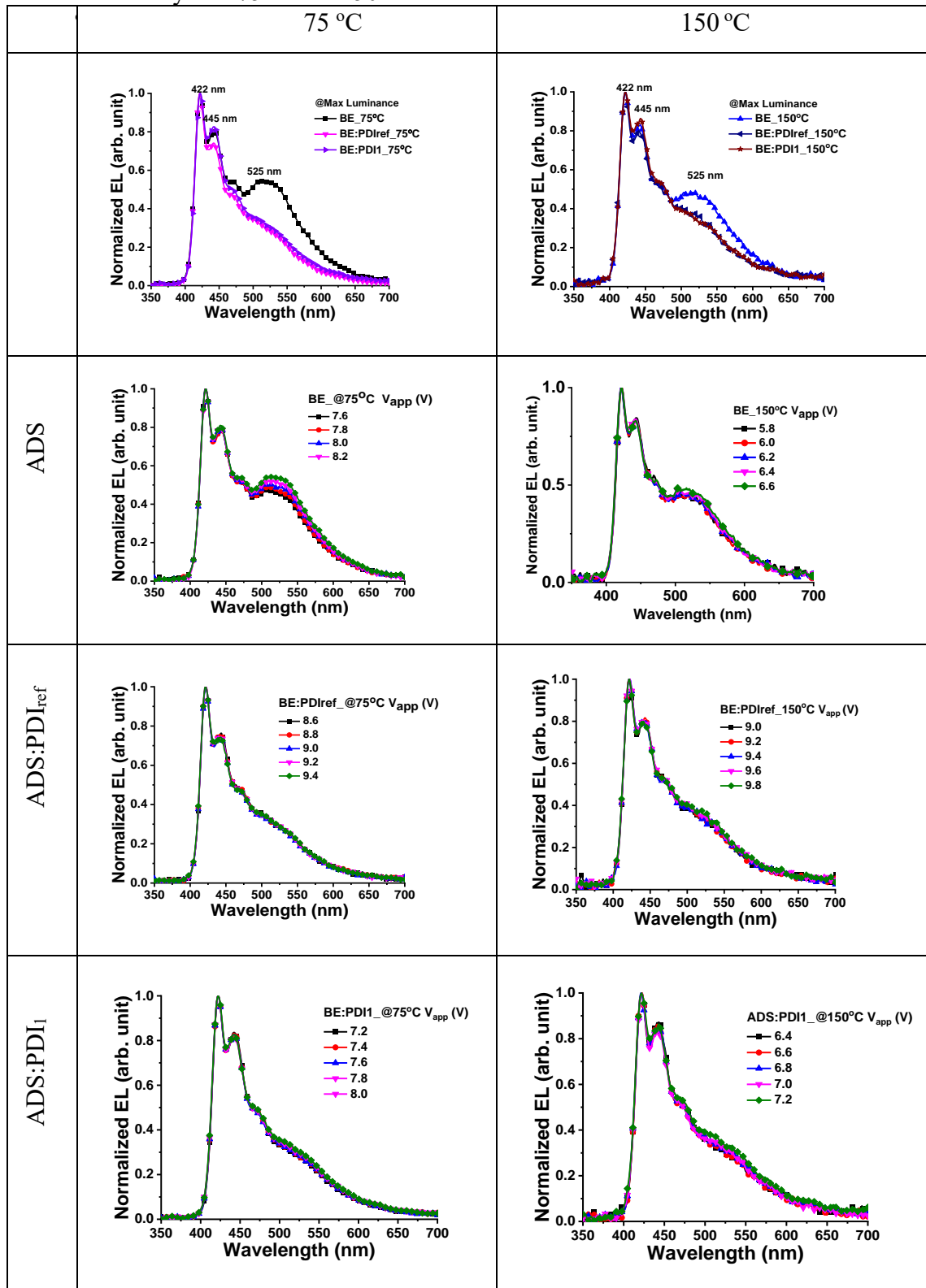
A.2. a, e) current density, b, f) luminescence vs voltage and, c, g) current efficiency and d, h) power efficiency vs current density characteristics of devices prepared by coating with chlorobenzene and toluene solvent and annealed at different temperatures in N₂ atmosphere, respectively.



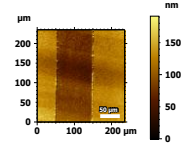
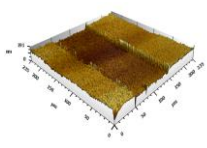
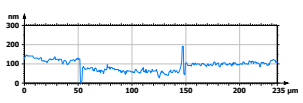
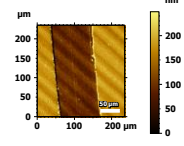
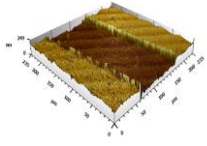
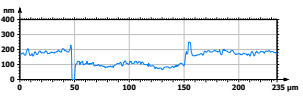
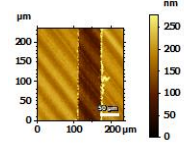
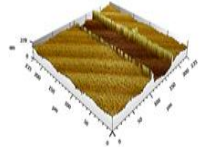
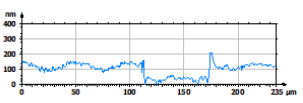
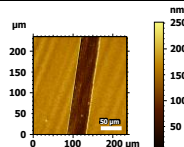
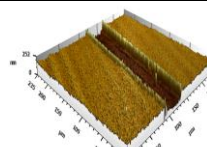
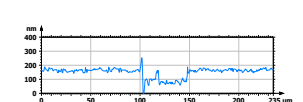
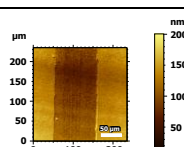
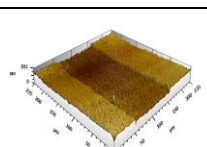
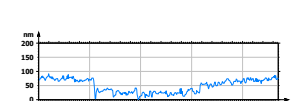
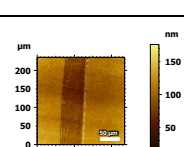
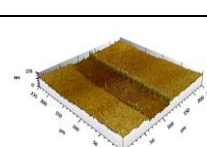

A.3. a) current density, b) luminescence vs voltage and, c) current efficiency d) power efficiency, e) external quantum efficiency vs current density and f) normalized electroluminescence vs wavelength at maximum luminescence characteristics of devices prepared by coating prepared by BE and PDIs doped BE emissive layer.



A.4. Normalized electroluminescence vs wavelength at maximum electroluminescence characteristics of devices prepared by coating prepared by BE and PDIs doped BE emissive layer at 75°C and 150°C.



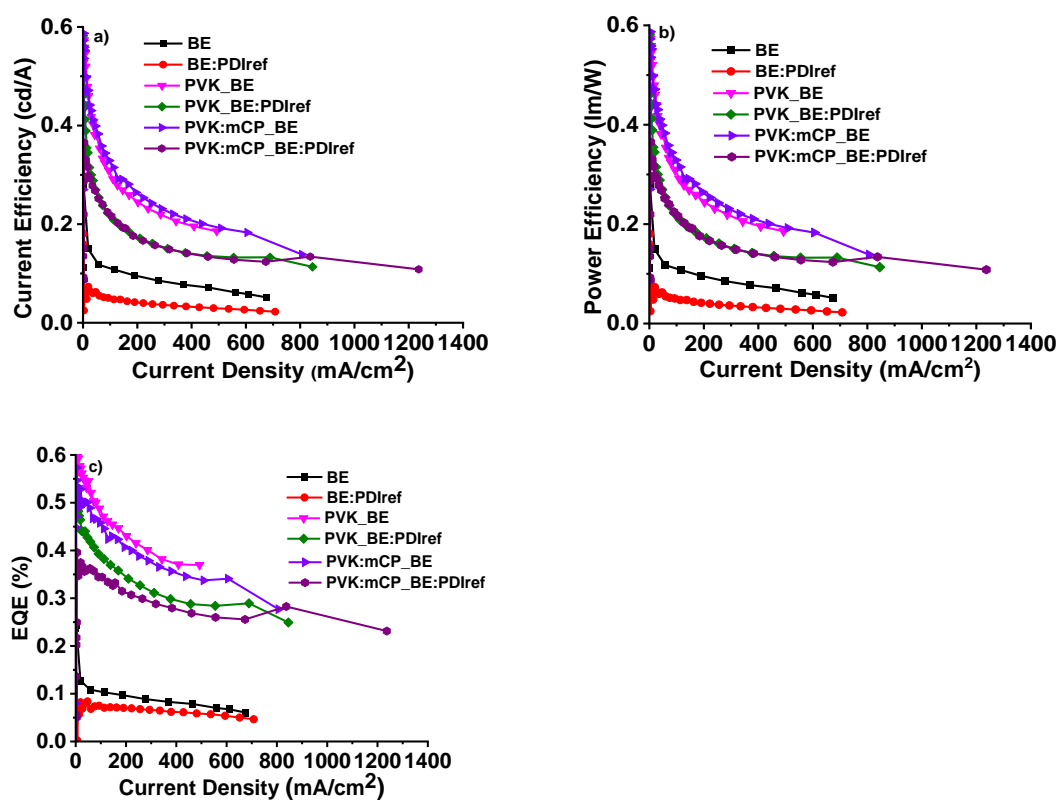
A.5. Film thickness measurements of the thin films of fabricated devices.

Material	2D	3D	Profile	Thickness (nm)
PEDOT:PSS 120°C				69.8 ± 3.2
BE (Tol) 150°C				85.3 ± 3
BE:PDI _{ref} (Tol) 150°C				86.5 ± 3
BE:PDI ₁ (Tol) 150°C				83.3 ± 3
PVK (CB) 150°C				59.1 ± 2
PVK:mCP (3:1) (CB) 150°C				53.0 ± 2

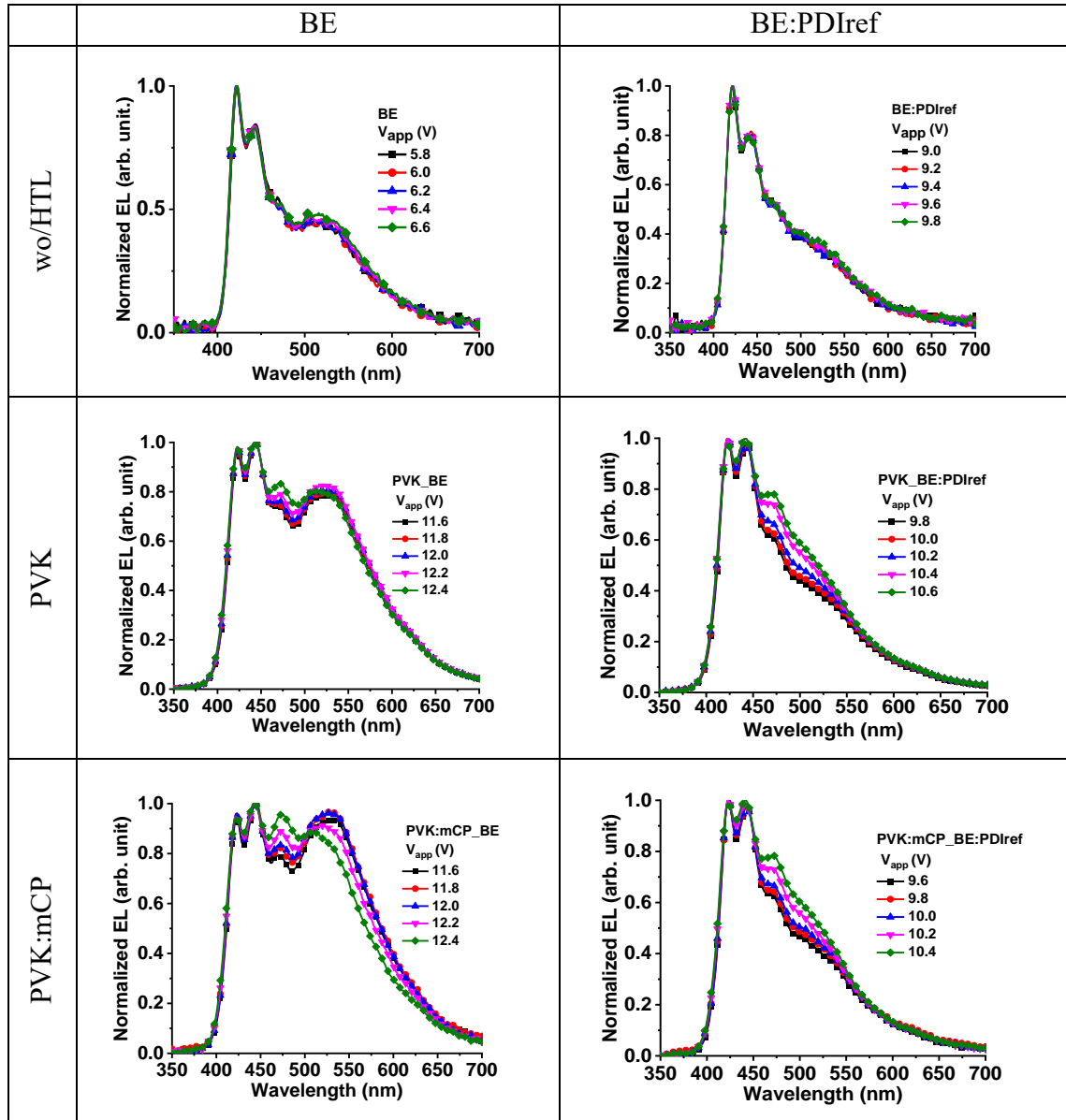
A.6 Energy bandgap and levels of organic semiconductors in produced devices.

Material	ΔE_{opt} (V)	HOMO (eV)	LUMO (eV)
mCP	3.5	-5.9	-2.4
PVK	3.6	-5.8	-2.2
ADS231BE	3.13	-5.75	-2.62
PDlref	2.28	-5.97	-3.69
PDI(2EH)-1	2.13	-5.87	-3.74

A.7 a) current efficiency b) power efficiency and c) external quantum efficiency vs current density characteristics of devices prepared by coating prepared by BE and PDIs doped BE emissive layer and PVK and PVK:mCP hole transfer layers.



A.8. Normalized electroluminescence vs wavelength at maximum electroluminescence characteristics of devices prepared by coating prepared by bare BE and PDlref doped BE emissive layer and PVK and PVK:mCP hole transfer layers.



A.9. Solid state Raman spectrum of a) 1550-1650 cm^{-1} , b) 1100-1500 cm^{-1} and c) 300-1100 cm^{-1} all active layer without and with HTL layers.

